Steroidogenesis and androgen/estrogen signaling pathways are altered in *in vitro* matured testicular tissues of prepubertal mice

Short title: *In vitro* testicular steroidogenesis

Laura Moutard[1], Caroline Goudin[1], Catherine Jaeger[1], Céline Duparc[1], Estelle Louiset[1], Tony Pereira[2], François Fraissinet[2], Marion Delessard[1], Justine Saulnier[1], Aurélie Rives-Feraille[1], Christelle Delalande[3], Hervé Lefebvre[1], Nathalie Rives[1], Ludovic Dumont[1], Christine Rondanino[1*].

[1] Univ Rouen Normandie, Inserm, NorDic, UMR 1239, Adrenal and Gonadal Pathophysiology team, F-76000 Rouen, France

[2]Department of General Biochemistry, Rouen University Hospital, F-76000 Rouen, France

[3]Normandie Univ, UNICAEN, OeReCa, F-14000 Caen

* **Corresponding author**: christine.rondanino@univ-rouen.fr

Key words: androgen, estrogen, *in vitro* spermatogenesis, Leydig cell, mice, steroidogenesis .

Abstract

Cancer treatments such as chemotherapy can have gonadotoxic effects. In order to preserve and restore the fertility of prepubertal patients with cancer, testicular biopsies are frozen and could theoretically be later matured *in vitro* to produce spermatozoa for assisted reproductive technology. A complete *in vitro* spermatogenesis has been obtained from prepubertal testicular tissue in the mouse model, although the sperm yield was low. Since steroid hormones play an essential role in spermatogenesis, it appears necessary to ensure that their synthesis and mechanisms of action are not altered in *in vitro* cultured tissues. The aim of this study was therefore to investigate steroidogenesis as well as androgen and estrogen signaling during *in vitro* maturation of mouse prepubertal testicular tissues.

Histological, RT-qPCR, Western blot analyses, measurements of cholesterol, steroid hormones levels and aromatase activity were performed on fresh or frozen/thawed *in vitro* cultured mouse testicular tissues from 6.5 days *postpartum* (d*pp*) mice as well as on age-matched *in vivo* controls.

A similar density of Leydig cells (LC) was found after 30 days of organotypic culture (D30) and at 36.5 d*pp*, the corresponding *in vivo* time point. However, LC were partially mature after *in vitro* culture, with decreased *Sult1e1* and *Insl3* mRNA levels (adult LC markers). Moreover, the transcript levels of *Cyp11a1*, *Cyp17a1* and *Hsd17b3* encoding steroidogenic enzymes were decreased *in vitro*. Increased amounts of progesterone and estradiol and reduced androstenedione intratesticular levels were observed at D30. Furthermore, androgen signaling was altered at D30, with decreased transcript levels of androgen target genes (*Rhox5*, *Septin12*). Moreover, the expression and activity of aromatase and estrogen signaling were impaired at D30. The addition of hCG to the organotypic culture medium induced an elevation in androgen production but did not improve sperm yield.

In conclusion, this study reports partial LC maturation, disturbed steroidogenic activity of LC, abnormal steroid hormone content as well as altered androgen and estrogen signaling in cultures of fresh and frozen/thawed prepubertal mouse testicular tissues. The organotypic culture system will need to be further improved to increase the efficiency of *in vitro* spermatogenesis and allow a clinical application.

Introduction

Pediatric cancer treatments such as chemotherapy have recognized toxicity on germline stem cells, which could lead to infertility at adulthood [1,2]. In order to preserve and restore male fertility, fragments of prepubertal testicular tissue are frozen and could theoretically be later matured to produce spermatozoa for assisted reproductive technology procedures. So far, fertility restoration approaches have not been clinically validated. *In vitro* maturation strategies are currently being developed and optimized in animal models. *In vitro* spermatogenesis could indeed be proposed to patients with testicular localization of residual tumor cells, for whom testicular tissue autografting is not indicated (about 30% of patients with acute leukemia). The organotypic culture procedure, which preserves testicular tissue architecture, microenvironment and cell interactions, has been used successfully to obtain spermatozoa from fresh or frozen/thawed mouse prepubertal testicular tissues [3–6]. In addition, viable and fertile mice have been obtained from *in vitro* produced spermatozoa by oocyte microinjection [3,4].

It has been previously shown that supplementing organotypic culture media with 1 µM retinol improves the *in vitro* production of spermatids and spermatozoa in prepubertal mouse testicular tissues cultured at a gas-liquid interphase [5,7]. However, *in vitro* sperm production still remains a rare event. A decreased expression of the androgen receptor (AR)-regulated gene *Rhox5* at the end of the culture period was evidenced, suggesting that testosterone production by Leydig cells (LC) and/or AR transcriptional activity could be impaired in organotypic cultures [8]. A decline in intratesticular testosterone levels has been highlighted during the first wave of mouse *in vitro* spermatogenesis [9]. Apart from that, whether LC maturation and functionality are affected in organotypic cultures has been poorly explored so far.

LC populations that differentiate during the prenatal and postnatal period are identified as Fetal Leydig cells (FLC) and Adult Leydig cells (ALC), respectively. Although FLC and ALC commonly express the majority of steroidogenic proteins required for androgen production, such as steroidogenic acute regulatory protein (StAR), P450 side chain cleavage (CYP11A1), 3β-hydroxysteroid dehydrogenase (3β-HSD) and P450 17α-hydroxylase/C17-20 lyase (CYP17A1), several genes are differentially expressed in the two LC populations [10]. Notably, 17β-hydroxysteroid dehydrogenase type 3 (17β-HSD3), an enzyme involved in the last step of testosterone biosynthesis, is expressed only by ALC, and not by FLC. Consequently, the major androgens produced in FLC and ALC are androstenedione and testosterone, respectively [10,11].

In rodents, the ALC lineage can be divided into four distinct stages: stem, progenitor, immature and adult [12]. Stem Leydig cells (SLC) express stem cell markers but do not express the LC lineage biomarkers, such as LHCGR, StAR or 3β-HSD [13]. Progenitor Leydig cells (PLC) are morphologically similar to the undifferentiated SLC but express LC markers, such as the steroidogenic enzymes CYP11A1 and CYP17A1 and do not express 17β-HSD3 [14]. However, PLC express high levels of androgen metabolizing enzymes, 5α-reductase 1 (SRD5A1) and 3α-hydroxysteroid dehydrogenase (3α-HSD) [15,16]. The differentiation of SLC into PLC is induced by the pituitary gonadotropin LH (Luteinizing Hormone) and by IGF1 (Insulin-like Growth Factor 1) [17]. Then, the activities of CYP11A1, 3β-HSD, and CYP17A1 increase in immature Leydig cells (ILC) as they mature from PLC [16]. ILC begin to express 17β-HSD3 and therefore can synthetize testosterone from androstenedione [16]. However, ILC still have high levels of SRD5A1 and 3α-HSD [16]. Adult Leydig cells (ALC) have increased expression of CYP11A1, 3β-HSD, CYP17A1, and 17β-HSD3. At this stage, SRD5A1 and 3α-HSD expression being silenced [16], testosterone is the major androgen [16]. ALC also express and secrete high levels of INSL3 under the

regulation of AR [18]. Furthermore, ALC express specifically SULT1E1 [19], which protects LC and seminiferous tubules against estrogen overstimulation by catalyzing the sulfoconjugation and inactivation of estrogens [20]. The proliferation and differentiation of the LC lineage are regulated by different factors, such as DHH and IGF1. DHH is required for both proliferation and differentiation of SLC into ALC [21]. IGF1 stimulates the proliferation of PLC and ILC [17] and promotes the maturation of ILC into ALC [22].

The steroid hormones produced by LC are essential for the progression of spermatogenesis. Testosterone, synthesized under the control of LH, is involved in spermatogonial proliferation and differentiation, meiotic progression, spermiogenesis and germ cell survival [23]. Androgen-binding protein (ABP), produced by Sertoli cells under the regulation of FSH, increases the accumulation of androgens in the seminiferous epithelium and makes them available for binding to intracellular AR [24]. Estrogens, derived from the aromatization of androgens by CYP19A1 (aromatase) in somatic and germ cells, regulate spermatogonial proliferation as well as spermatocyte and spermatid apoptosis [25]. The expression of aromatase is age-dependent, being mostly in Sertoli cells in immature rodent testes and then in LC during adulthood. In mouse, aromatase is also present within seminiferous tubules, mainly in spermatids. The expression of this enzyme is enhanced by the pituitary gonadotropins FSH and LH and its activity is stimulated by LH and its homologue hCG (human Chorionic Gonadotropin) [26].

Androgens and estrogens act locally on somatic and/or germ cells expressing their receptors (AR and ERα, ERβ, GPER, respectively) to regulate the expression of target genes. *Septin12*, encoding a filament forming protein present in the acrosome, is a direct target gene of testosterone in post-meiotic germ cells [27], but also of estrogens, with 2 ERα and 1 AR binding sites in its promoter [28]. *Rhox5*, encoding a transcription factor involved in germ cell survival, and *Eppin*, encoding a serine protease inhibitor, are two other target genes of

testosterone in Sertoli cells, with androgen response elements (ARE) in their promoters [29]. *Faah*, encoding a hydrolase that protects Sertoli cells from apoptosis, is a direct target gene of estrogens in mature Sertoli cells [30]. Its promoter activity engages ERβ and the histone demethylase LSD1 [30].

Since steroid hormones play an essential role in the progression of spermatogenesis, it appears necessary to ensure that their syntheses and mechanisms of action are not altered in *in vitro* cultured testicular tissues. The aim of the present work was therefore to study LC maturation, steroidogenesis and androgen/estrogen signaling in a comprehensive manner during the *in vitro* maturation of mouse prepubertal testicular tissues.

Materials and methods

Ethical approval

All the experimental procedures were approved by the Institutional Animal Care and Use Committee of Rouen Normandy University under the licence/protocol number APAFiS #38239.

Mice and testis collection

CD-1 mice (Charles River Laboratories, L'Arbresle, France) were housed in a temperature-controlled room (22–23°C) under a 12-h light/dark cycle. Prepubertal 6.5-day *postpartum* (d*pp*) male mice were euthanized by decapitation and underwent a bilateral orchidectomy. Testes were transferred to Petri dishes containing α-MEM without phenol red (Gibco by Life Technologies, Saint-Aubin, France) and the complete removal of the tunica albuginea was performed with two needles under a binocular magnifier (S8AP0, Leica Microsystems GmbH, Wetzlar, Germany). Testes were then either cultured immediately (culture from fresh tissues), or after a freezing/thawing cycle (**S1 Fig**). Moreover, mice aged 22.5 and 36.5 d*pp* were

euthanized by CO_2 asphyxiation and their testes were used as *in vivo* controls for 16 and 30 days of culture, respectively (**S1 Fig**).

Controlled slow freezing (CSF) and thawing of testicular tissues

Freezing procedure

Testes were placed into cryovials (Dominique Dutscher, Brumath, France) containing 1.5 mL of the following cryoprotective medium: Leibovitz L15 medium (Eurobio, Courtabœuf, France) supplemented with 1.5 M dimethylsulfoxyde (DMSO, Sigma-Aldrich, Saint-Quentin Fallavier, France), 0.05 M sucrose (Sigma-Aldrich), 10% (v/v) fetal calf serum (FCS, Life Technologies) and 3.4 mM vitamin E (Sigma-Aldrich) [31]. After a 30-min equilibration at 4°C, samples were frozen in a programmable freezer (Nano Digitcool, CryoBioSystem, L'Aigle, France) with a CSF protocol: start at 5°C, then -2°C/min until reaching -9°C, stabilization at -9°C for 7 min, then -0.3°C/min until -40°C and -10°C/min down to -140°C. Testicular tissues were then plunged and stored in liquid nitrogen.

Thawing procedure

Cryotubes were warmed for 1 min at room temperature (RT) and then for 3 min in a water bath at 30°C. They were then successively incubated at 4°C in solutions containing decreasing concentrations of cryoprotectants for 5 min each [solution 1: 1 M DMSO, 0.05 M sucrose, 10% FCS, 3.4 mM vitamin E, Leibovitz L15; solution 2: 0.5 M DMSO, 0.05 M sucrose, 10% FCS, 3.4 mM vitamin E, Leibovitz L15; solution 3: 0.05 M sucrose, 10% FCS, 3.4 mM vitamin E, Leibovitz L15; solution 4: 10% FCS, 3.4 mM vitamin E, Leibovitz L15].

Organotypic cultures at a gas–liquid interphase

In vitro tissue cultures were performed as previously described [3,5]. Briefly, prepubertal 6.5-day old mouse testes, which contain spermatogonia as the most advanced type of germ cells, were first cut into four fragments. They were placed on top of two 1.5% (w/v) agarose Type I gels (Sigma-Aldrich) half-soaked in medium. Testicular tissues were then cultured under 5%

CO_2 at 34°C for 16 days (D16), which corresponds to the end of meiosis and the appearance of the first round spermatids, or 30 days (D30) to explore the end of the first spermatogenic wave. The basal medium (BM) contained α-MEM without phenol red, 10% KSR (KnockOut Serum Replacement, Gibco by Life Technologies), 0.1 mg/mL streptomycin and 100 UI/mL penicillin (Sigma-Aldrich). The medium was chosen without phenol red because of its estrogen activity [32]. Retinol (10^{-6} M, Sigma-Aldrich) is added in all organotypic cultures from D2 and then every 8 days in order to respect the meiosis entry cycle of spermatogonia [5]. Furthermore, the basal medium was supplemented or not with 1 nM hCG (MSD France, Courbevoie, France) from D16 in order to assess LC functionality. Media were prepared just before use and were replaced twice a week.

Histological analyses

Tissue fixation, processing and sectioning

Testicular tissues were fixed with Bouin's solution (Sigma-Aldrich) or 4% paraformaldehyde (PFA, Sigma-Aldrich) for 2 h at room temperature. They were then dehydrated in ethanol in the Citadel 2000 tissue processor (Shandon, Cheshire, UK) and embedded in paraffin. Tissue sections (3 µm thick) were prepared with the RM2125 RTS microtome (Leica) and were mounted on Polysine slides (Thermo Fisher Scientific, Waltham, MA, USA).

Periodic Acid Schiff (PAS) reaction

A PAS reaction was then performed on *in vitro* matured tissues. Tissue sections were deparaffinized in xylene and rehydrated in decreasing concentrations of ethanol. Slides were then immersed in 0.5% periodic acid (Thermo Fisher Scientific) for 10 min, rinsed for 5 min in water and then placed for 30 min in the Schiff reagent (Merck, Darmstadt, Germany). After three 2-min washes in water, sections were counterstained with Mayer's hematoxylin and mounted with Eukitt (CML, Nemours, France). Images were acquired on a DM4000B microscope (Leica) at a ×400 magnification. The most advanced type of germ cells present in

the testicular fragments was analyzed in at least 30 cross-sectioned seminiferous tubules from 2 sections with the Application Suite Core v2.4 software (Leica).

Immunofluorescence staining

After deparaffinization, rehydration and a 3-min wash in phosphate buffered saline (PBS, Sigma-Aldrich), tissue sections were boiled in 10 mM citrate buffer pH 6.0 (Diapath, Martinengo, Italy) for 40 min at 96°C. They were cooled for 20 min at RT and rinsed in distilled water for 5 min. A permeabilization step with 0.1% (v/v) Triton X-100 (Sigma-Aldrich) was performed at RT for 15 min for Ki67/3β-HSD immunostaining. Non-specific sites were blocked with 5% (w/v) bovine serum albumin (BSA, Sigma-Aldrich) and 5% (v/v) horse serum (Sigma-Aldrich). Slides were then incubated in humidified environment with primary antibodies (**S1 Table**), rinsed 3 times in PBST (PBS with 0.05% Tween-20) and incubated with appropriate secondary antibodies (**S1 Table**). For Ki67/3β-HSD, a sequential protocol was performed as follows: incubation with anti-Ki67 antibodies overnight at 4°C, incubation with secondary antibodies coupled to Alexa 594 for 60 min at RT, fixation with 4% PFA for 15 min at RT and incubation with anti-3β-HSD antibodies directly coupled to Alexa 488 for 90 min at RT. Sections were washed, dehydrated with ethanol and mounted in Vectashield with Hoechst. Images were acquired on a THUNDER Imager 3D Tissue microscope (Leica) at a ×400 magnification. LC number (3β-HSD^{+}) was normalized to tissue area (cm^2).

Immunohistochemical staining

After deparaffinization and rehydration, endogenous peroxidases were blocked with HP Block (Dako, Les Ulis, France) for 30 min and non-specific binding sites were blocked with Ultra-V Block solution (Thermo Fisher Scientific) for 10 min at RT. Tissue sections were then incubated overnight at 4°C with anti-CYP19A1 antibodies (**S1 Table**). After three 5-min washes in PBS, they were incubated for 10 min at RT with biotinylated polyvalent secondary

antibodies (UltraVision Detection System HRP kit, Thermo Fisher Scientific). After three 5-min washes in PBS, a 10-min incubation at RT with streptavidin associated with peroxidase (UltraVision Detection System HRP kit, Thermo Fisher Scientific) was performed. The labeling was revealed after application of a chromogenic substrate (EnVision FLEX HRP Magenta Chromogen, Dako) for 10 min at RT.

RNA extraction and RT-qPCR

RNA extraction

Total RNA was extracted from testicular samples using RNeasy Micro kit (Qiagen, Courtabœuf, France) according to the manufacturer's instructions. For *in vitro* cultured tissues, the central necrotic area was carefully removed before RNA extraction. To avoid contamination with genomic DNA, extracted RNA was incubated with two units of TURBO DNase (Life Technologies) for 45 min at 37°C. The amount of the RNA samples was measured with a NanoDrop Spectrophotometer (NanoDrop Technologies, Wilmington, DE, USA) and purity was determined by calculating the ratio of optical densities at 260 nm and 280 nm.

Reverse transcription

The reverse transcription reaction was performed in a 96-well plate from 1 µg total RNA with 4 µL of qScript cDNA SuperMix 5X (QuantaBiosciences, Gaithersburg, MD, USA) and ribonuclease-free water to adjust the volume to 20 µL. Reverse transcription was performed according to the following program: 5 min at 25°C, 30 min at 42°C and 5 min at 85°C. The complementary DNA (cDNA) obtained were diluted 1:10.

Polymerase chain reaction

cDNA amplifications were carried out in a total volume of 13 µL containing 6 ng of cDNA templates, 6.5 µL of SYBR Green (Thermo Fisher Scientific) and 300 nM of each primer. Specific primers are listed in **S2 Table**. Samples were dispensed using the Bravo pipetting

robot (Agilent Technologies, Santa Clara, CA, USA). Reactions were performed in 384-well plates (Life Technologies) in a Quant Studio 12K Flex system. The amplification condition was 20 s at 95°C followed by 40 cycles (1 s at 95°C, 20 s at 60°C) and a final step of denaturation of 15 s at 95°C, 1 min at 60°C and 15 s at 95°C. Melting curves were obtained to ensure the specificity of PCR amplifications. The size of the amplicons was verified by agarose gel electrophoresis (E-gel 4%, Life Technologies). The relative expression level of each gene was normalized to two housekeeping genes as recommended by the MIQE guidelines [33]: *Gapdh* and *Actb*, which were identified and validated as the most stable and suitable genes for RT-qPCR analysis in mouse testis development [34]. 3β-hydroxysteroid dehydrogenase (*Hsd3b1*), a selective LC marker, has been used as a normalization factor for the analysis of genes expressed in LC [35]. Data were analyzed using the $2^{-\Delta\Delta Ct}$ method [36].

Western Blot

Protein extraction

Testes were homogenized in ice-cold RIPA buffer (50 mM Tris HCl, 0.5% cholic acid, 0.1% SDS, 150 mM NaCl) containing a protease inhibitor cocktail (Sigma-Aldrich). For *in vitro* cultured tissues, the central necrotic area was carefully removed before protein extraction.

Determination of protein concentration by the Bradford method

Total protein concentration was measured in the homogenates. The assay was performed in a 96-well plate in a final volume of 200 µL containing the sample and Bradford's solution (BioRad, Marnes-la-Coquette, France). After a 5-min incubation at RT, the optical density at 595 nm was measured using a Spark spectrophotometer (Tecan, Lyon, France).

Western Blot

Protein extracts (20 µg) were separated on 12% resolving polyacrylamide gels (BioRad) and transferred onto nitrocellulose membranes (BioRad). The membranes were blocked with 5% milk or 5% BSA in TBST (0.2% Tween-20 in Tris Buffered Saline) for 30 min at 37°C before

incubation overnight at 4°C with the appropriate primary antibody (**S1 Table**). After washes, membranes were incubated with the appropriate HRP-conjugated secondary antibodies (**S1 Table**). ECL reagents (BioRad) were used to detect the immunoreactivity. Images were captured with the ChemiDoc XRS+ Imaging System (BioRad). Densitometric analyses were performed using Image Lab™ v5.0 software (BioRad) and protein levels were normalized to β-actin.

Intratesticular cholesterol levels

Total testicular lipids were extracted from ~10 mg tissue with a Lipid Extraction kit (ab211044; Abcam, Paris, France) according to the manufacturer's instructions. Dried lipid extracts were reconstituted in 200 µL of assay buffer. Intratesticular levels of total, free, and esterified cholesterol were measured with a colorimetric Cholesterol/Cholesteryl Ester assay kit (ab65359; Abcam) according to the manufacturer's instructions.

Hormonal assays

Sample preparation for liquid chromatography coupled to mass spectrometry (LC-MS/MS)

Testicular fragments were homogenized in 200 µL (6.5 d*pp* tissues and *in vitro* matured tissues) or 400 µL (22.5 d*pp* and 36.5 d*pp* tissues) of 0.1 M phosphate buffer pH 7.4 with a cocktail of protease inhibitors (Sigma-Aldrich). Total protein concentration was measured as described above.

LC-MS/MS

The standards for androstenedione, testosterone, dehydroepiandrosterone (DHEA) and their stable labeled isotopes were obtained from Merck. Working solutions were prepared in methanol. Serial dilutions from working solutions were used to prepare seven-point calibration curves and 3 quality control levels for all analytes. For the final calibration and quality control solutions, PBS was used for testicular fragments and α-MEM for medium. The

linearity ranges were from 0.05 to 10 ng/mL for androstenedione and testosterone, and from 1 to 200 ng/mL for DHEA. A simple deproteinization was carried out by automated sample preparation system, the CLAM-2030 (Shimadzu Corporation, Marne-la-Vallée, France) coupled to a 2D-UHPLC-MS/MS system. Once the sample on board, 30 µL was automatically pipetted in a pre-conditioned tube containing a filter, in which reagents were added, then mixed and filtered. Briefly, the polytetrafluoroethylene (PTFE) filter vial (0.45 µm pore size) was previously conditioned with 20 µL of methanol (Carlo Erba, Val-de-Reuil, France). Successively, 30 µL of sample and 60 µL of a mixture of isotopically labeled internal standards in acetonitrile were added. The mixture was agitated for 120 s (1900 rpm), then filtered by application of vacuum pressure (-60 to -65 kPa) for 120 s into a collection vial. Finally, 30 µL of the extract was injected in the 2D-UHPLC-MS/MS system.

Analysis was performed on a two dimensions ultra-performance liquid chromatograph-tandem mass spectrometer (2D-UHPLC-MS/MS) consisting of the following Shimadzu® modules (Shimadzu Corporation): an isocratic pump LC20AD SP, for pre-treatment mode, a binary pump consisting of coupling two isocratic pumps Nexera LC30AD for the analytical mode, an automated sampler SIL-30AC, a column oven CTO-20AC and a triple-quadrupole mass spectrometer LCMS-8060. The assay was broken down into two stages. The first was the pre-treatment where the sample was loaded on the perfusion column. The second step was the elution of the compounds of interest to the analytical column. The deproteinized extract performed by the CLAM-2030 was automatically transferred to the automated sampler, where 30 µL was directly analyzed into the chromatographic system. The LC-integrated online sample clean-up was performed using a perfusion column Shimadzu® MAYI-ODS (5 mm L × 2 mm I.D.). The first step consisted of loading the extract on the perfusion column with a mobile phase composed of 10 mM ammonium formate in water (Carlo Erba) at a flow rate of 0.5 mL/min during 2 min. Then the system switched to the analytical step to elute the analytes

from the perfusion column to the analytical column to achieve chromatographic separation. During this step, the loading line was washed with propan-2-ol (Carlo Erba) during 3 min. Chromatographic separation was achieved on a Restek® Raptor Biphenyl (50 mm L × 3 mm I.D. , 2.7 µm) maintained at 40 °C and a gradient of (A) 1 mM ammonium fluoride buffer in water (Carlo Erba) and (B) methanol (Carlo Erba) at a flow rate of 0.675 mL/min as follows: 0.0–2.10 min, 5% (B); 2.1–3.0 min, 5 to 65% (B); 3.0–4.75 min, 65% (B); 4.75–5.0 min, 65 to 70% (B); 5.0–6.6 min, 70% (B); 6.6–8.0, 70 to 75% (B); 8.0–8.5 min, 75 to 100% (B); 8.50–9.5 min, 100% (B); 9.5–9.6 min, 100% to 5% (B); 9.6–12.0 min, 5% (B). Detection and quantification were performed by scheduled- Multiple Reaction Monitoring (MRM) using 1 ms pause time and 50 ms dwell times to achieve sufficient points per peak. The interface parameters and common settings were as follows: interface voltage: 1 kV; nebulizing gas flow: 3 L/min; heating gas flow: 10 L/min; drying gas flow: 10 L/min; interface temperature: 400 °C; desolvation line (DL) temperature: 150 °C; heat block temperature: 500 °C; collision gas pressure 300 kPa. Compound-specific MRM parameters are shown in **S3 Table**.

Enzyme-linked immunosorbent assay (ELISA)

Steroids were extracted from testicular homogenates and from organotypic culture media with 5 volumes of diethyl ether (Carlo Erba). The organic phase was then recovered and evaporated in a water bath at 37°C. The tubes were stored at -20°C until use.

Progesterone and estradiol levels were measured in 50 µL of testicular homogenates and in 50 µL of culture media using Cayman ELISA kit (582601 for progesterone and 501890 for estradiol, Cayman Chemical Company, Ann Arbor, MI, USA), according to the supplier's recommendations. The sensitivity limit for the progesterone assay was 10 pg/mL with average intra- and inter-trial variations of 13.9% and 9.6%, respectively. The sensitivity limit for the estradiol assay was 20 pg/mL and the lower limit of detection was 6 pg/mL with average intra- and inter-trial variations of 20.25% and 14.975%, respectively.

Aromatase activity

After homogenization of ~10-50 mg of tissues in 500 µL of Aromatase Assay Buffer, the aromatase activity was measured with the fluorometric Aromatase (CYP19A) Activity assay kit (ab273306; Abcam) according to the manufacturer's instructions.

Radioimmunoassay (RIA)

INSL3 was assayed by using RIA kit with ^{125}I as tracer (RK-035-27, Phoenix Pharmaceuticals, Strasbourg, France). According to the manufacturer's instructions, analyses were performed on 100 µL of culture media or tissue homogenates. Assay validation was assessed by determining the recovery of expected amounts of INSL3 in samples to which exogenous INSL3 was added. The sensitivity of the INSL3 RIA kit was 60.4 pg/mL and the range of the assay was 10-1280 pg/mL.

Statistical analyses

Statistical analyses were carried out with GraphPad Prism 8 software (GraphPad Software Inc., La Jolla, CA, USA). Data are presented as means ± SEM. The non-parametric Mann-Whitney test was used to compare *in vitro* cultures and *in vivo* controls; cultures of fresh and CSF tissues; cultures with or without hCG. A value of $P < 0.05$ was considered statistically significant.

Results

Leydig cells (LC) are present after 30 days of organotypic culture but are partially mature

3β-HSD immunofluorescence staining was first performed to detect and quantify LC during mouse postnatal development and in *in vitro* cultured fresh testicular tissues (FT). The percentage of LC in apoptosis or in proliferation was measured after cleaved caspase 3 or Ki67 immunofluorescence staining respectively, and the percentage of LC expressing AR,

which is required for their proliferation and maturation [37], was also determined. The transcript levels of genes involved in LC differentiation (*Igf1*, *Dhh*) and of FLC (*Mc2r*), ILC (*Srd5a1*), or ALC (*Sult1e1*, *Insl3*) markers were then assessed by RT-qPCR. Finally, the concentration of INSL3, a marker of LC maturity, was also measured by RIA in organotypic culture media and in testicular homogenates.

After 16 days of culture, the number of LC per cm² of testicular tissue was not significantly different from 22.5 d*pp*, the age-matched *in vivo* control (**Fig 1A-B**). However, at this time point, the percentage of apoptotic LC was increased compared to the *in vivo* control while the percentage of proliferating LC was unchanged (**Fig 1C**). In addition, the percentage of LC expressing AR was similar at D16 and 22.5 d*pp* (**Fig 1D**). Whereas no difference was observed in the mRNA levels of *Dhh*, *Srd5a1* and *Sult1e1* between D16 and 22.5 d*pp*, *Igf1* and *Insl3* transcripts levels were respectively higher and lower in 16-day organotypic cultures than *in vivo* (**Fig 1E**). *Mc2r* transcripts were barely detected at D16 and 22.5 d*pp* as well as at later time points, thereby reflecting the low amount of FLC in prepubertal testicular tissues (data not shown).

After 30 days of culture, no significant difference in the number of LC per cm² of testicular tissue and in the percentages of apoptotic and proliferating LC was observed compared to 36.5 d*pp*, the corresponding *in vivo* time point (**Fig 1A-C**). Furthermore, the percentage of LC expressing AR was comparable after *in vitro* or *in vivo* maturation (**Fig 1D**). The transcript levels of *Dhh* were also similar in *in vitro* and *in vivo* matured tissues at the end of the first spermatogenic wave (**Fig 1E**). However, a reduction in the mRNA levels of *Igf1*, *Srd5a1* and the two ALC markers (*Sult1e1*, *Insl3*) was found at D30 in comparison to 36.5 d*pp in vivo* controls (**Fig 1E**). Moreover, intratesticular INSL3 was below the detection limit (<10 pg/mL) in *in vitro* matured tissues (**Fig 1F**) and a significant elevation in the concentration of INSL3 was observed in culture medium from D22 to D30 for FT tissues ($P = 0.0002$; **Fig 1F**).

Controlled slow freezing has no impact on LC density or maturity before or after organotypic culture

In the clinics, testicular biopsies from prepubertal boys are frozen and stored in liquid nitrogen for later use. In order to assess the impact of freezing/thawing procedures (CSF) on LC in organotypic cultures, we conducted the same analyses as above on 6.5 d*pp* CSF mouse testicular tissues and on *in vitro* matured 6.5 d*pp* CSF tissues (**S2 Fig**).

CSF had no impact on the number of LC per cm² of tissue at 6.5 d*pp* as well as after 16 or 30 days of culture (**S2A-B Fig**). Although the percentage of apoptotic LC was lower in CSF than in FT tissues at 6.5 d*pp*, it was similar in CSF and FT tissues at D16 and D30 (**S2C Fig**). Furthermore, no change in the percentage of LC in proliferation or expressing AR was found after CSF (**S2C-D Fig**). Moreover, LC differentiation factors and markers were expressed at similar levels in CSF and FT tissues (**S2E Fig**), expect for *Igf1* transcript levels which were decreased in CSF tissues at D16 and for *Insl3* transcript levels which were higher in CSF than in FT tissues at D16 and D30 (**S2E Fig**).

The expression of several actors of steroidogenesis is affected in organotypic cultures

The transcript levels of several genes involved in steroidogenesis were then measured by RT-qPCR during mouse postnatal development and in *in vitro* cultured testicular tissues to determine the testicular steroidogenic potential of cultured tissues (**Fig 2A**). The protein levels of two steroidogenic enzymes, 3β-HSD and CYP17A1, were also quantified by Western Blot (**Fig 2A**).

Controlled slow freezing had no impact on the mRNA levels of all the genes examined at 6.5 d*pp*, *i.e.* before culture (**Fig 2A**). At D16, the mRNA levels of *Star*, *Cyp17a1* and *Hsd17b3* were decreased in FT and CSF testicular tissues compared to 22.5 d*pp* testes (**Fig 2A**). *Cyp11a1* transcript levels were also lower in FT tissues at D16 than at 22.5 d*pp* (**Fig**

2A). In contrast, *Lhcgr*, *Hsd3b1* and *Hsd17b2* transcript levels remained unchanged at this time point (**Fig 2A**). While 3β-HSD protein levels were not different between D16 and 22.5 d*pp*, CYP17A1 protein levels were found to be decreased only in FT tissues at D16 compared to 22.5 d*pp* (**Fig 2A**).

The mRNA levels of *Cyp11a1*, *Hsd3b1*, *Cyp17a1*, *Hsd17b3* and *Hsd17b2* were lower at D30 in both FT and CSF tissues than in the physiological situation (**Fig 2A**). Despite a significant decrease in *Hsd3b1* mRNA levels at D30, the protein levels of 3β-HSD were not significantly different after 30 days of culture and at 36.5 d*pp* (**Fig 2A**). Western blot experiments however showed that the expression of CYP17A1 was also reduced at the protein level in both FT and CSF tissues at D30 compared to 36.5 d*pp* (**Fig 2A**). This steroidogenic enzyme was still detectable by immunofluorescence in Leydig cells in cultured tissues (**Fig 2B**). Finally, *Lhcgr* and *Star* mRNA levels were found significantly reduced at D30 in FT and CSF tissues, respectively (**Fig 2A**).

Increased intratesticular concentrations of progesterone and estradiol combined with decreased intratesticular concentration of androstenedione in organotypic cultures

We then wondered whether the production of steroids was altered in *in vitro* cultured testicular tissues. To answer this question, the concentrations of androstenedione, DHEA and testosterone were measured by LC-MS/MS and the concentrations of progesterone and estradiol were assessed by ELISA in both testicular samples and the culture media (**Fig 3**). DHEA was below the detection limit (<1 ng/mL) in all the samples examined (data not shown). The intratesticular concentrations of progesterone were significantly increased at D16 and D30 in both FT and CSF tissues compared to their respective *in vivo* controls (**Fig 3A**). In contrast, the intratesticular concentrations of androstenedione were significantly decreased at D16 in both FT and CSF tissues and at D30 in FT tissues compared to *in vivo* controls (**Fig**

3B). The intratesticular concentrations of testosterone were however not different in *in vitro* and *in vivo* matured tissues at both time points (**Fig 3C**). In addition, the intratesticular concentrations of estradiol were significantly higher at D16 and D30 in FT and CSF tissues than in their respective *in vivo* controls (**Fig 3D**).

In the organotypic culture medium, a significant increase in the concentrations of progesterone was observed at D26 only (242.5 ± 37.95 pg/mL) (P = 0.0417; **Fig 3E**). Furthermore, a significant elevation in the concentrations of androstenedione was observed from D16 (0.658 ± 0.056 ng/mL) to D30 (3.285 ± 0.364 ng/mL) (P < 0.0001; **Fig 3E**). Regarding testosterone, following a decrease in the levels of this androgen in the culture media between D2 (16.615 ± 0.819 ng/mL) and D14 (5.628 ± 0.365 ng/mL) (P = 0.0020), an augmentation was then detected between D26 (8.025 ± 1.321 ng/mL) and D30 (17.9 ± 5.458 ng/mL) (P = 0.0078; **Fig 3E**). At D30, the concentrations of both androstenedione and testosterone were higher in the culture media of FT tissues than of CSF tissues (**S3 Fig**). Regarding estradiol, no significant change in its concentrations was observed in the media between D6 and D30 (**Fig 3E**).

Since steroids are derived from cholesterol, intratesticular levels of total, free and esterified cholesterol were also analyzed during mouse postnatal development and in *in vitro* cultured testicular tissues (**Fig 3F**). Controlled slow freezing had no impact on cholesterol levels at 6.5 d*pp*, *i.e.* before culture (**Fig 3F**). The intratesticular levels of esterified cholesterol were comparable between the different experimental conditions (**Fig 3F**). However, total cholesterol levels were higher in FT and CSF cultured tissues at D16 and D30 compared to their corresponding *in vivo* time points (**Fig 3F**). Moreover, free cholesterol levels were increased in FT and CSF cultured tissues at D30 compared to 36.5 d*pp* and in FT tissues at D16 (**Fig 3F**).

Androgen and estrogen signaling are altered in 30-day organotypic cultures

The mRNA levels of actors of androgen and estrogen signaling were next measured by RT-qPCR (**Figs 4 and 5**). The protein expression of the androgen receptor (AR), aromatase (CYP19) and fatty acid amide hydrolase (FAAH whose expression is regulated by estrogen) was also assessed by Western Blot (**Figs 4 and 5**).

The transcript levels of *Ar*, encoding the androgen receptor, were higher at D16 in FT tissues than at 22.5 d*pp* but were not significantly different between D30 and 36.5 d*pp* (**Fig 4A**). Conversely, AR protein levels were comparable at D16 in FT tissues and 22.5 d*pp* but were more elevated at D30 in both FT and CSF tissues than at 36.5 d*pp* (**Fig 4A**). Our immunofluorescence data showed that AR was expressed in Sertoli cells, peritubular myoid cells and Leydig cells in 16-day and 30-day cultured tissues as well as in the corresponding *in vivo* controls (**Fig 4B**). The transcript levels of three AR-regulated genes (*Rhox5*, *Septin12*, *Eppin*) were decreased in FT and CSF tissues cultured for 16 days compared to 22.5 d*pp* (**Fig 4C**). At D30, *Rhox5* and *Septin12* mRNA levels were still lower than *in vivo* while *Eppin* mRNA levels were higher than at 36.5 d*pp* (**Fig 4C**). In addition, a significant increase in *Abp* mRNA levels was found at D30 in CSF but not in FT tissues, while no difference was found at earlier time points (**Fig 4C**).

Intriguingly, the expression of *Cyp19a1*, encoding aromatase, was drastically diminished after 30 days of culture in FT and CSF tissues compared to 36.5 d*pp* (**Fig 5A**). The protein levels of CYP19 were found reduced in both FT and CSF tissues at D16 and D30 (**Fig 5A**). CYP19 was expressed in Leydig cells at 6.5 d*pp* and was then found in elongated spermatids and spermatozoa at 36.5 d*pp*, whereas no expression could be detected in cultured testes (**Fig 5B**). CYP19 enzymatic activity was also significantly decreased in CSF cultures at D30 (**Fig 5C**). In addition, the transcript levels of the three genes encoding estrogen receptors (*Esr1*, *Esr2*,

Gper1) and of the estrogen target gene *Faah* were significantly lower at D30 than at 36.5 d*pp* (**Fig 5D-E**). *Esr1* mRNA levels were also decreased at D16 (**Fig 5D**). FAAH protein levels were decreased in 16-day FT and 30-day CSF organotypic cultures (**Fig 5E**).

Leydig cells are functional as they respond to hCG stimulation

We examined the impact of hCG supplementations (5 pM, 50 pM, 1 nM, 5 nM or 50 nM) on the intratesticular concentrations of testosterone and the secretion of this hormone in the organotypic culture medium. Since the concentration of hCG leading to the best response (*i.e.* plateau of the dose-response curves for intratesticular and secreted testosterone) was 1 nM, we used this dose for the rest of the analyses (**S4 Fig**).

Upon supplementation with 1 nM hCG, intratesticular androstenedione levels were significantly increased at D30 in FT but not CSF tissues (**Fig 6A**). The intratesticular testosterone levels were higher at D30 in both FT and CSF tissues following hCG supplementation (**Fig 6A**). Moreover, a significant increase in androstenedione and testosterone concentrations was observed in the culture media of both FT and CSF tissues following hCG supplementation (**Fig 6A**). The amounts of androgens released into the culture media were however lower for CSF tissues than for FT tissues (**Fig 6A**).

The addition of 1 nM hCG had no impact on the transcript levels of *Hsd17b3*, *Hsd3b1*, *Ar* and *Esr1* in both FT and CSF cultures. *Hsd17b3* and *Esr1* mRNA levels still remained lower upon hCG supplementation than *in vivo* (**Fig 6B**). No effect of hCG was also observed in FT cultures for *Star*, *Faah*, *Srd5a1*, *Sult1e1*, *Dhh*, *Abp* and *Hsd17b2* mRNA levels (**Fig 6B**, **S5 Fig**). *Lhcgr*, *Cyp11a1*, *Cyp17a1*, *Cyp19a1*, *Esr2*, *Gper1* and *Insl3* mRNA levels were increased after hCG supplementation in FT cultures (**Fig 6B, S5 Fig**). Whereas *Cyp11a1*, *Cyp17a1* and *Cyp19a1* mRNA levels were still lower after hCG supplementation than *in vivo*, *Esr2* and *Gper1* transcripts were restored to their physiological levels (**Fig 6B**). In contrast, mRNA levels of *Rhox5*, *Eppin*, *Septin12* and *Igf1* were decreased after hCG supplementation

in FT cultures, with *Rhox5*, *Septin12* and *Igf1* transcript levels lower than those observed *in vivo* (**Fig 6B, S5 Fig**).

Finally, the mean proportions of seminiferous tubules reaching the round spermatid and elongated spermatid stages were lower in tissues cultured with than without hCG (**Fig 6C**). The number of Sertoli cells inside seminiferous tubules was unchanged following hCG supplementation, but was higher than in *in vivo* controls (**Fig 6D**).

Discussion

The present study shows for the first time and in a comprehensive manner that LC maturation and functionality as well as steroid hormone signaling are impaired in cultures of fresh and frozen/thawed immature mouse testes. Only few differences were found between fresh and frozen/thawed *in vitro* matured tissues.

A similar density of LC was found in organotypic cultures and in corresponding *in vivo* controls. However, LC only partially matured *in vitro*. At D16, the expression of the LC differentiation factors *Igf1* and *Dhh* was unaffected. At D30, the proliferation/apoptosis balance was undisturbed in LC while the expression of *Insl3* was faint, as well as that of *Sult1e1*, another LC maturity marker. The deficient LC maturation observed at D30 could be related to the decreased levels of *Igf1*, which encodes insulin-like growth factor 1 known to promote the maturation of ILC into ALC [22]. Indeed, the labeling index of ILC and ALC was previously found to be reduced in *Igf1*$^{-/-}$ mouse testes between 21 and 56 d*pp* [17].

LC functionality was also altered in organotypic cultures. Indeed, the expression of several genes encoding steroidogenic enzymes (*Cyp11a1*, *Cyp17a1*, *Hsd17b3*, *Hsd17b2*) was downregulated in these cells at D30 (**Fig 7**). Decreased *Cyp11a1* and *Cyp17a1* transcript levels were also previously reported in *Igf1*$^{-/-}$ mice, together with decreased intratesticular testosterone levels [17]. Furthermore, deficiency in insulin-like growth factors signaling in *Insr*$^{-/-}$/*Igf1r*$^{-/-}$ mouse LC was shown to impair testicular steroidogenesis (decreased *Lhcgr*,

Star, *Cyp11a1*, *Cyp17a1*, *Hsd17b3*, *Srd5a1* and *Insl3* mRNA levels) and increase estradiol production [38]. Here, we report for the first time an accumulation of estradiol in *in vitro* cultured tissues, which could be deleterious for sperm production. To promote LC maturation and lower intratesticular estradiol levels *in vitro*, supplementation of culture medium with IGF1 could thus be later envisaged, and even more so since this factor has been shown to increase, although modestly, the percentages of round and elongated spermatids in cultured mouse testicular fragments [39]. To reduce estrogen levels and increase sperm production, supplementation of the organotypic culture medium with selective estrogen receptor modulators (SERMs) such as tamoxifen or with aromatase inhibitors such as letrozole could also be considered in future studies. These molecules have indeed proven to be effective in increasing sperm concentration in infertile men [40–42].

Our work also revealed an elevation in progesterone and a reduction in androstenedione in *in vitro* matured tissues (**Fig 7**), which could arise from the collapsed expression of *Cyp17a1*. A greater sperm production has been highlighted in PRKO mice (lacking the progesterone receptor), thereby showing the inhibitory action of progesterone on spermatogenesis [43]. Furthermore, progesterone alone or in combination with estradiol can have inhibitory effects on spermatogenesis in rats [44]. The cumulative excess of progesterone and estradiol in cultured testicular tissues may therefore slow the progression of *in vitro* spermatogenesis and lead to a poor sperm yield.

Despite the disturbed steroidogenic activity of LC *in vitro*, the accumulation of estradiol and progesterone, the decrease in androstenedione, and in contradiction with a previous study [9], intratesticular testosterone levels in cultured tissues were not significantly different from *in vivo*. Moreover, a complete *in vitro* spermatogenesis was achieved, albeit with a low efficiency as previously described [5,6]. We also found that the percentage of LC expressing AR was unchanged under *in vitro* conditions. The increased AR protein levels at D30 could

thus be the result of the higher number of Sertoli cells within seminiferous tubules. Intriguingly, common points can be observed in our organotypic cultures and in LCARKO (LC-specific *Ar*$^{-/-}$) mice [45]: decreased *Insl3*, *Cyp17a1* and *Hsd17b3* mRNA levels, increased intratesticular progesterone levels and unchanged intratesticular testosterone levels compared to *in vivo* controls. This could suggest that AR signaling is dysfunctional in LC *in vitro*. The downregulation of *Rhox5* expression (**Fig 7**), which confirms our previous findings [8], further suggests that AR signaling may also be impaired in Sertoli cells. Recently, in a mouse model with disrupted dimerization of the AR ligand-binding-domain, a decreased expression of *Hsd17b3* and of AR-regulated genes, such as *Rhox5* and *Insl3*, a higher percentage of Sertoli cells and a decreased production of round and elongated spermatids were found [46], which further supports our hypothesis that AR signaling may be defective in organotypic cultures. In the SPARKI (SPecificity-affecting AR KnockIn)-AR mouse model, which has a defect in binding to AR-specific DNA motifs while displaying normal interaction with the classical androgen response elements (AREs), it has been shown that *Rhox5* expression is regulated by an AR-selective ARE, while *Eppin* expression is regulated by a classical, nonselective ARE [47]. The differential regulation of these two androgen-responsive genes could explain why *Rhox5* mRNA levels were downregulated while *Eppin* mRNA levels were upregulated in our cultures. We also report here that the transcript levels of *Septin12*, another androgen target gene, was reduced *in vitro* (**Fig 7**). As *Septin12* is expressed by post-meiotic germ cells [27], the decrease of its expression may be the result of their low numbers in cultures.

Additionally, estrogen signaling was impaired in organotypic cultures, with a low expression of the estrogen-synthesizing enzyme aromatase, of estrogen receptors and of the estrogen target gene *Faah* (**Fig 7**). Since the expression of *Cyp19a1*, *Esr1* and *Esr2* (encoding aromatase, ERα and ERβ, respectively) can be downregulated by estradiol in the rat testis

[48,49], we hypothesize that the transcription of these genes may be negatively controlled by elevated estradiol levels in our tissue cultures. *Faah*, whose promoter activity engages ERβ and the histone demethylase LSD1, is a direct target gene of estrogens in Sertoli cells [30]. The *Faah* proximal promoter is not regulated by estrogen in immature Sertoli cells, as they express ERβ at the same level as mature cells but do not express LSD1 [30]. Thus, the decreased *Faah* transcript levels in organotypic cultures could be the consequence of the downregulated ERβ expression and/or of the immaturity of Sertoli cells. Whether Sertoli cells in organotypic cultures are as mature as *in vivo* is unknown and will be the focus of future studies. The transcription of *Insl3*, which is repressed by estradiol in a MA-10 Leydig cell line model [50], could also be inhibited by the excess of estradiol in our tissue cultures. Interestingly, our *in vitro* cultured testes exhibit common features with the testes of *Sult1e1*$^{-/-}$ mice lacking estrogen sulfotransferase, an enzyme that catalyzes the sulfoconjugation and inactivation of estrogens [20]: decreased *Cyp17a1* expression as well as increased progesterone levels and local estrogen activity [51,52]. The remaining question in our case is whether estrogen excess is the cause or the consequence of low *Sult1e1* expression.

Finally, as previously reported [5,6], the presence of LH or its homologue hCG was not necessary to reconstitute a full first spermatogenic wave *in vitro*. However, plasma LH concentration is known to rise *in vivo* from 21-28 d*pp* in the mouse model [53]. We previously showed that the addition of 0.075 nM (50 IU/L) hCG together with FSH from D7 onwards modestly increased the number of spermatozoa produced in organotypic cultures [5]. To mimic as closely as possible the physiological conditions, 1 nM hCG was added in the culture medium from D16 onwards. Even though LC responded to this stimulation by synthesizing and secreting more androgens, supplementation of the culture medium with 1 nM hCG alone was not sufficient to increase the yield of *in vitro* spermatogenesis.

In conclusion, the present study shows the partial maturation and the disturbed steroidogenic activity of LC, the abnormal steroid hormone content as well as the altered androgen and estrogen signaling in organotypic cultures of fresh and frozen/thawed prepubertal mouse testicular tissues. Altogether, these defects could contribute to the low efficiency of *in vitro* spermatogenesis. Before clinical applications can be envisaged, the organotypic culture system will therefore have to be further optimized.

Conflict of Interest

The authors declare that the research was conducted in the absence of any commercial or financial relationships that could be construed as a potential conflict of interest.

Author Contributions

LM conceived the design of the study, led experiments, acquired, analyzed and interpreted data, and drafted the manuscript. CG, CJ, CD, EL, TP, FF, CD and LD contributed to the experiments and data collection. MD, JS, ARF, LD and CR provided advices during the experimental phase and discussion of the results. NR and CR designed the project. CR and LD corrected the manuscript. HL, NR and CR acquired funding. NR, LD and CR supervised the study. All the authors read and approved the final manuscript.

Funding

This work was supported by a PhD grant from Région Normandie (awarded to LM) and by fundings from Ligue contre le Cancer Comité de Seine-Maritime (awarded to CR), France Lymphome Espoir (Bourse Sacha awarded to CR), Région Normandie and Europe (RIN Steroids awarded to HL) and ANR (ANR-21-CE14-0068, sc-SpermInVitro awarded to NR).

The funders had no role in study design, data collection and analysis, decision to publish, or preparation of the manuscript.

Acknowledgements

Data from RT-qPCR and images were obtained on PRIMACEN (http://www.primacen.fr), the Cell Imaging Platform of Normandy, IRIB, Faculty of Sciences, University of Rouen, 76821 Mont-Saint-Aignan. The authors also thank the U1096 team for the access to their Western Blot devices.

References

1. Allen CM, Lopes F, Mitchell RT, Spears N. How does chemotherapy treatment damage the prepubertal testis? Reproduction. 2018; R209–R233. doi:10.1530/REP-18-0221

2. Miller KD, Siegel RL, Lin CC, Mariotto AB, Kramer JL, Rowland JH, et al. Cancer treatment and survivorship statistics, 2016. CA: A Cancer Journal for Clinicians. 2016;66: 271–289. doi:10.3322/caac.21349

3. Sato T, Katagiri K, Gohbara A, Inoue K, Ogonuki N, Ogura A, et al. In vitro production of functional sperm in cultured neonatal mouse testes. Nature. 2011;471: 504–507. doi:10.1038/nature09850

4. Yokonishi T, Sato T, Komeya M, Katagiri K, Kubota Y, Nakabayashi K, et al. Offspring production with sperm grown in vitro from cryopreserved testis tissues. Nat Commun. 2014;5: 4320. doi:10.1038/ncomms5320

5. Arkoun B, Dumont L, Milazzo J-P, Way A, Bironneau A, Wils J, et al. Retinol Improves In Vitro Differentiation of Pre-Pubertal Mouse Spermatogonial Stem Cells into Sperm during the First Wave of Spermatogenesis. Schlatt S, editor. PLoS ONE. 2015;10: e0116660. doi:10.1371/journal.pone.0116660

6. Dumont L, Arkoun B, Jumeau F, Milazzo J-P, Bironneau A, Liot D, et al. Assessment of the optimal vitrification protocol for pre-pubertal mice testes leading to successful in vitro production of flagellated spermatozoa. Andrology. 2015;3: 611–625. doi:10.1111/andr.12042

7. Dumont L, Oblette A, Rondanino C, Jumeau F, Bironneau A, Liot D, et al. Vitamin A prevents round spermatid nuclear damage and promotes the production of motile sperm during *in vitro* maturation of vitrified pre-pubertal mouse testicular tissue. Mol Hum Reprod. 2016; molehr;gaw063v2. doi:10.1093/molehr/gaw063

8. Rondanino C, Maouche A, Dumont L, Oblette A, Rives N. Establishment, maintenance and functional integrity of the blood–testis barrier in organotypic cultures of fresh and frozen/thawed prepubertal mouse testes. MHR: Basic science of reproductive medicine. 2017;23: 304–320. doi:10.1093/molehr/gax017

9. Pence LM, Schmitt TC, Beger RD, Del Valle PL, Nakamura N. Testicular function in cultured postnatal mouse testis fragments is similar to that of animals during the first wave of spermatogenesis. Birth Defects Research. 2019;111: 270–280. doi:10.1002/bdr2.1451

10. O'Shaughnessy PJ, Johnston H, Willerton L, Baker PJ. Failure of normal adult Leydig cell development in androgen-receptor-deficient mice. J Cell Sci. 2002;115: 3491–3496.

11. Shima Y, Miyabayashi K, Haraguchi S, Arakawa T, Otake H, Baba T, et al. Contribution of Leydig and Sertoli Cells to Testosterone Production in Mouse Fetal Testes. Molecular Endocrinology. 2013;27: 63–73. doi:10.1210/me.2012-1256

12. Ye L, Li X, Li L, Chen H, Ge R-S. Insights into the Development of the Adult Leydig Cell Lineage from Stem Leydig Cells. Front Physiol. 2017;8: 430. doi:10.3389/fphys.2017.00430

681 13. Jiang MH, Cai B, Tuo Y, Wang J, Zang ZJ, Tu X, et al. Characterization of Nestin-positive stem
682 Leydig cells as a potential source for the treatment of testicular Leydig cell dysfunction. Cell
683 Res. 2014;24: 1466–1485. doi:10.1038/cr.2014.149

684 14. Oh YS, Koh IK, Choi B, Gye MC. ESR1 inhibits hCG-induced steroidogenesis and proliferation of
685 progenitor Leydig cells in mice. Sci Rep. 2017;7: 43459. doi:10.1038/srep43459

686 15. Mahendroo M, Wilson JD, Richardson JA, Auchus RJ. Steroid 5α-reductase 1 promotes 5α-
687 androstane-3α,17β-diol synthesis in immature mouse testes by two pathways. Molecular and
688 Cellular Endocrinology. 2004;222: 113–120. doi:10.1016/j.mce.2004.04.009

689 16. Ge R-S, Hardy MP. Variation in the End Products of Androgen Biosynthesis and Metabolism
690 during Postnatal Differentiation of Rat Leydig Cells*. Endocrinology. 1998;139: 3787–3795.
691 doi:10.1210/endo.139.9.6183

692 17. Hu G-X, Lin H, Chen G-R, Chen B-B, Lian Q-Q, Hardy DO, et al. Deletion of the Igf1 gene:
693 suppressive effects on adult Leydig cell development. J Androl. 2010;31: 379–387.
694 doi:10.2164/jandrol.109.008680

695 18. Ivell R, Alhujaili W, Kohsaka T, Anand-Ivell R. Physiology and evolution of the INSL3/RXFP2
696 hormone/receptor system in higher vertebrates. General and Comparative Endocrinology.
697 2020;299: 113583. doi:10.1016/j.ygcen.2020.113583

698 19. Sararols P, Stévant I, Neirijnck Y, Rebourcet D, Darbey A, Curley MK, et al. Specific
699 Transcriptomic Signatures and Dual Regulation of Steroidogenesis Between Fetal and Adult
700 Mouse Leydig Cells. Front Cell Dev Biol. 2021;9: 695546. doi:10.3389/fcell.2021.695546

701 20. Song W-C. The Role of Estrogen Sulfotransferase in Leydig Cells. In: Payne AH, Hardy MP,
702 editors. The Leydig Cell in Health and Disease. Totowa, NJ: Humana Press; 2007. pp. 197–205.
703 doi:10.1007/978-1-59745-453-7_14

704 21. Li X, Wang Z, Jiang Z, Guo J, Zhang Y, Li C, et al. Regulation of seminiferous tubule-associated
705 stem Leydig cells in adult rat testes. Proc Natl Acad Sci USA. 2016;113: 2666–2671.
706 doi:10.1073/pnas.1519395113

707 22. Chamindrani Mendis-Handagama SML, Siril Ariyaratne HB. Differentiation of the Adult Leydig
708 Cell Population in the Postnatal Testis. Biology of Reproduction. 2001;65: 660–671.
709 doi:10.1095/biolreprod65.3.660

710 23. O'Shaughnessy PJ. Hormonal control of germ cell development and spermatogenesis. Seminars
711 in Cell & Developmental Biology. 2014;29: 55–65. doi:10.1016/j.semcdb.2014.02.010

712 24. Hansson V, Weddington SC, French FS, McLean W, Smith A, Nayfeh SN, et al. Secretion and role
713 of androgen-binding proteins in the testis and epididymis. J Reprod Fertil Suppl. 1976; 17–33.

714 25. Zanatta AP, Brouard V, Gautier C, Goncalves R, Bouraïma-Lelong H, Mena Barreto Silva FR, et al.
715 Interactions between oestrogen and 1α,25(OH)2-vitamin D3 signalling and their roles in
716 spermatogenesis and spermatozoa functions. Basic Clin Androl. 2017;27: 10.
717 doi:10.1186/s12610-017-0053-z

718 26. Carreau S. Leydig Cell Aromatase. In: Payne AH, Hardy MP, editors. The Leydig Cell in Health
719 and Disease. Totowa, NJ: Humana Press; 2007. pp. 189–195. doi:10.1007/978-1-59745-453-
720 7_13

721 27. Lin Y-H, Lin Y-M, Wang Y-Y, Yu I-S, Lin Y-W, Wang Y-H, et al. The Expression Level of Septin12 Is
722 Critical for Spermiogenesis. The American Journal of Pathology. 2009;174: 1857–1868.
723 doi:10.2353/ajpath.2009.080955

724 28. Kuo P-L, Tseng J-Y, Chen H-I, Wu C-Y, Omar HA, Wang C-Y, et al. Identification of SEPTIN12 as a
725 novel target of the androgen and estrogen receptors in human testicular cells. Biochimie.
726 2019;158: 1–9. doi:10.1016/j.biochi.2018.11.018

727 29. De Gendt K, McKinnell C, Willems A, Saunders PTK, Sharpe RM, Atanassova N, et al.
728 Organotypic Cultures of Prepubertal Mouse Testes: A Method to Study Androgen Action in
729 Sertoli Cells while Preserving their Natural Environment. Biology of Reproduction. 2009;81:
730 1083–1092. doi:10.1095/biolreprod.109.078360

731 30. Grimaldi P, Pucci M, Di Siena S, Di Giacomo D, Pirazzi V, Geremia R, et al. The faah gene is the
732 first direct target of estrogen in the testis: role of histone demethylase LSD1. Cell Mol Life Sci.
733 2012;69: 4177–4190. doi:10.1007/s00018-012-1074-6

734 31. Milazzo JP, Vaudreuil L, Cauliez B, Gruel E, Masse L, Mousset-Simeon N, et al. Comparison of
735 conditions for cryopreservation of testicular tissue from immature mice. Human Reproduction.
736 2008;23: 17–28. doi:10.1093/humrep/dem355

737 32. Berthois Y, Katzenellenbogen JA, Katzenellenbogen BS. Phenol red in tissue culture media is a
738 weak estrogen: implications concerning the study of estrogen-responsive cells in culture. Proc
739 Natl Acad Sci USA. 1986;83: 2496–2500. doi:10.1073/pnas.83.8.2496

740 33. Bustin SA, Benes V, Garson JA, Hellemans J, Huggett J, Kubista M, et al. The MIQE Guidelines:
741 Minimum Information for Publication of Quantitative Real-Time PCR Experiments. Clinical
742 Chemistry. 2009;55: 611–622. doi:10.1373/clinchem.2008.112797

743 34. Gong Z-K, Wang S-J, Huang Y-Q, Zhao R-Q, Zhu Q-F, Lin W-Z. Identification and validation of
744 suitable reference genes for RT-qPCR analysis in mouse testis development. Mol Genet
745 Genomics. 2014;289: 1157–1169. doi:10.1007/s00438-014-0877-6

746 35. Cacciola G, Chioccarelli T, Altucci L, Ledent C, Mason JI, Fasano S, et al. Low 17beta-Estradiol
747 Levels in Cnr1 Knock-Out Mice Affect Spermatid Chromatin Remodeling by Interfering with
748 Chromatin Reorganization. Biology of Reproduction. 2013;88: 152–152.
749 doi:10.1095/biolreprod.112.105726

750 36. Livak KJ, Schmittgen TD. Analysis of Relative Gene Expression Data Using Real-Time
751 Quantitative PCR and the 2−ΔΔCT Method. Methods. 2001;25: 402–408.
752 doi:10.1006/meth.2001.1262

753 37. O'Shaughnessy PJ, Mitchell RT, Monteiro A, O'Hara L, Cruickshanks L, der Grinten HC, et al.
754 Androgen receptor expression is required to ensure development of adult Leydig cells and to
755 prevent development of steroidogenic cells with adrenal characteristics in the mouse testis.
756 BMC Dev Biol. 2019;19: 8. doi:10.1186/s12861-019-0189-5

757 38. Radovic Pletikosic SM, Starovlah IM, Miljkovic D, Bajic DM, Capo I, Nef S, et al. Deficiency in
758 insulin-like growth factors signalling in mouse Leydig cells increase conversion of testosterone
759 to estradiol because of feminization. Acta Physiol. 2021;231. doi:10.1111/apha.13563

760 39. Yao J, Zuo H, Gao J, Wang M, Wang D, Li X. The effects of IGF-1 on mouse spermatogenesis
761 using an organ culture method. Biochemical and Biophysical Research Communications.
762 2017;491: 840–847. doi:10.1016/j.bbrc.2017.05.125

763 40. Cannarella R, Condorelli RA, Mongioì LM, Barbagallo F, Calogero AE, La Vignera S. Effects of the
764 selective estrogen receptor modulators for the treatment of male infertility: a systematic
765 review and meta-analysis. Expert Opinion on Pharmacotherapy. 2019;20: 1517–1525.
766 doi:10.1080/14656566.2019.1615057

767 41. Kooshesh L, Bahmanpour S, Zeighami S, Nasr-Esfahani MH. Effect of Letrozole on sperm
768 parameters, chromatin status and ROS level in idiopathic Oligo/Astheno/Teratozoospermia.
769 Reprod Biol Endocrinol. 2020;18: 47. doi:10.1186/s12958-020-00591-2

770 42. Shuling L, Sie Kuei ML, Saffari SE, Jiayun Z, Yeun TT, Leng JPW, et al. Do men with normal
771 testosterone–oestradiol ratios benefit from letrozole for the treatment of male infertility?
772 Reproductive BioMedicine Online. 2019;38: 39–45. doi:10.1016/j.rbmo.2018.09.016

773 43. Lue Y, Wang C, Lydon JP, Leung A, Li J, Swerdloff RS. Functional role of progestin and the
774 progesterone receptor in the suppression of spermatogenesis in rodents. Andrology. 2013;1:
775 308–317. doi:10.1111/j.2047-2927.2012.00047.x

776 44. Adeoye O, Alex N, Sikiru B, Amos M, Opeyemi A. Studies of Estrogen and Progesterone on
777 Testicular Functions in Male Wistar Rats (Rattus Novergicus). EJMR. 2017;4.
778 doi:10.24041/ejmr2017.43

779 45. O'Hara L, McInnes K, Simitsidellis I, Morgan S, Atanassova N, Slowikowska-Hilczer J, et al.
780 Autocrine androgen action is essential for Leydig cell maturation and function, and protects
781 against late-onset Leydig cell apoptosis in both mice and men. FASEB j. 2015;29: 894–910.
782 doi:10.1096/fj.14-255729

783 46. El Kharraz S, Dubois V, Royen ME, Houtsmuller AB, Pavlova E, Atanassova N, et al. The androgen
784 receptor depends on ligand-binding domain dimerization for transcriptional activation. EMBO
785 Rep. 2021;22. doi:10.15252/embr.202152764

786 47. Schauwaers K, De Gendt K, Saunders PTK, Atanassova N, Haelens A, Callewaert L, et al. Loss of
787 androgen receptor binding to selective androgen response elements causes a reproductive
788 phenotype in a knockin mouse model. Proc Natl Acad Sci USA. 2007;104: 4961–4966.
789 doi:10.1073/pnas.0610814104

790 48. Zanatta AP, Gonçalves R, Ourique da Silva F, Pedrosa RC, Zanatta L, Bouraïma-Lelong H, et al.
791 Estradiol and 1α,25(OH)2 vitamin D3 share plasma membrane downstream signal transduction
792 through calcium influx and genomic activation in immature rat testis. Theriogenology.
793 2021;172: 36–46. doi:10.1016/j.theriogenology.2021.05.030

794 49. Genissel C, Levallet J, Carreau S. Regulation of cytochrome P450 aromatase gene expression in
795 adult rat Leydig cells: comparison with estradiol production. Journal of Endocrinology.
796 2001;168: 95–105. doi:10.1677/joe.0.1680095

797 50. Laguë É, Tremblay JJ. Estradiol represses Insulin-like 3 expression and promoter activity in MA-
798 10 Leydig cells. Toxicology. 2009;258: 101–105. doi:10.1016/j.tox.2009.01.013

799 51. Qian YM, Sun XJ, Tong MH, Li XP, Richa J. Targeted Disruption of the Mouse Estrogen
800 Sulfotransferase Gene Reveals a Role of Estrogen Metabolism in Intracrine and Paracrine
801 Estrogen Regulation. 2001; 9.

802 52. Tong MH, Christenson LK, Song W-C. Aberrant Cholesterol Transport and Impaired
803 Steroidogenesis in Leydig Cells Lacking Estrogen Sulfotransferase. Endocrinology. 2004;145:
804 2487–2497. doi:10.1210/en.2003-1237

805 53. Wu X, Arumugam R, Zhang N, Lee MM. Androgen profiles during pubertal Leydig cell
806 development in mice. REPRODUCTION. 2010;140: 113–121. doi:10.1530/REP-09-0349

807

Figure captions

Fig 1. Leydig cells are present after 30 days of organotypic culture but are partially mature. (A) Representative images of 3β-HSD expression by Leydig cells (LC) during mouse postnatal development (6.5 d*pp*, 22.5 d*pp* and 36.5 d*pp*) and in *in vitro* cultured tissues after 16 days of culture (D16) or 30 days (D30). Testicular tissue sections were counterstained with Hoechst (blue). Dotted lines delineate seminiferous tubules. Scale: 15 µm. (B) Number of 3β-HSD+ LC per cm² of testicular tissue during mouse postnatal development (6.5 d*pp*, 22.5 d*pp* and 36.5 d*pp*) and in *in vitro* cultured tissues (D16 and D30). (C) Percentage of LC in apoptosis (3β-HSD and cleaved caspase 3 positive) or in proliferation (3β-HSD and Ki67 positive) in *in vivo* and *in vitro* matured tissues. (D) Percentage of 3β-HSD positive LC expressing AR in *in vivo* and *in vitro* matured tissues. (E) Relative mRNA levels of differentiation factors for LC (*Igf1*, *Dhh*), ILC (*Srd5a1*) and ALC markers (*Sult1e1*, *Insl3*) (normalized to *Gapdh* and *Actb* or to *Hsd3b1*). (F) Intratesticular concentration of INSL3 (pg/mg of tissue) or in the culture medium (pg/mL).

Data are presented as means ± SEM with n = 4 biological replicates for each group. A value of $*P < 0.05$ was considered statistically significant. n.d.: not determined (under the detection limit)

FT: Fresh Tissue; CSF: Controlled Slow Freezing.

Fig 2. The expression of several actors of steroidogenesis is downregulated in 30-day organotypic cultures. (A) Relative mRNA levels of *Lhcgr*, *Star*, *Cyp11a1*, *Hsd3b1*, *Cyp17a1*, *Hsd17b3* and *Hsd17b2* (normalized to *Gapdh* and *Actb* or to *Hsd3b1*) and relative protein levels of 3β-HSD and CYP17A1 (normalized to ACTB) during mouse postnatal development (6.5 d*pp*, 22.5 d*pp* and 36.5 d*pp*) and in *in vitro* cultured FT or CSF tissues (D16 and D30). (B) Representative images of CYP17A1 expression during mouse postnatal development (22.5 d*pp* and 36.5 d*pp*) and in *in vitro* cultured tissues (D16 and D30). Testicular tissue sections were counterstained with Hoechst (blue). Dotted lines delineate seminiferous tubules. Scale: 15 µm.

Data are presented as means ± SEM with n = 4 biological replicates for each group. A value of $*P < 0.05$ was considered statistically significant.

Fig. 3: An increased production of progesterone and estradiol and a decreased production of androstenedione are observed after 16 and 30 days of culture of

prepubertal mouse testicular tissues. Intratesticular concentrations of (A) progesterone, (B) androstenedione, (C) testosterone and (D) estradiol during mouse postnatal development (6.5 d*pp*, 22.5 d*pp* and 36.5 d*pp*) and in *in vitro* cultured fresh (FT) or frozen/thawed (CSF) tissues (D16 and D30). Steroid concentrations were normalized to protein levels. (E) Concentrations of progesterone, androstenedione, testosterone and estradiol in the culture medium of FT tissues. (F) Intratesticular concentrations of total, free and esterified cholesterol normalized to tissue mass.

Data are presented as means ± SEM with n = 4 biological replicates for each group. A value of $*P < 0.05$ was considered statistically significant.

Fig. 4: Androgen signaling is altered in 30-day organotypic cultures. (A) Relative mRNA levels of *Ar* (normalized to *Gapdh* and *Actb*) and relative protein levels of AR (normalized to ACTB) during mouse postnatal development (6.5 d*pp*, 22.5 d*pp* and 36.5 d*pp*) and in *in vitro* cultured FT or CSF tissues (D16 and D30). (B) Representative images of AR expression at 22.5 d*pp* and 36.5 d*pp* and at corresponding *in vitro* time points (D16 and D30). Testicular tissue sections were counterstained with Hoechst (blue). Solid arrowheads: peritubular myoid cells. Open arrowheads: Sertoli cells. Arrows: Leydig cells. Dotted lines delineate seminiferous tubules (ST). Scale: 15 µm. (C) Relative mRNA levels of *Rhox5*, *Septin12*, *Eppin* and *Abp* (normalized to *Gapdh* and *Actb*).

Data are presented as means ± SEM with n = 4 biological replicates for each group. A value of $*P < 0.05$ was considered statistically significant.

Fig. 5: The expression of aromatase and estrogen signaling are impaired after 30 days of organotypic culture. (A) Relative mRNA levels of *Cyp19a1* (normalized to *Gapdh* and *Actb*) and relative protein levels of CYP19A1 (normalized to ACTB) during mouse postnatal development (6.5 d*pp*, 22.5 d*pp* and 36.5 d*pp*) and in *in vitro* cultured FT or CSF tissues (D16 and D30). The bands on the Western Blot correspond to different isoforms of CYP19. (B) Representative images of CYP19A1 expression at 6.5 d*pp*, 22.5 d*pp* and 36.5 d*pp* and at corresponding *in vitro* time points (D16 and D30). Testicular tissue sections were counterstained with Hematoxylin. Scale: 15 µm. Arrow: Leydig cells. Arrowheads: elongated spermatids. (C) Aromatase activity (normalized to tissue weight). (D) Relative mRNA levels of *Esr1*, *Esr2* and *Gper1* (normalized to *Gapdh* and *Actb*). (E) Relative mRNA levels of *Faah* (normalized to *Gapdh* and *Actb*) and relative protein levels of FAAH (normalized to ACTB). The second band at 80 kDa is an isoform of FAAH (Q8BRM1, UniProtKB).

Data are presented as means ± SEM with n = 4 biological replicates for each group. A value of *$P < 0.05$ was considered statistically significant.

Fig. 6: Leydig cells are functional as they respond to stimulation by 1 nM hCG. (A) Levels of androgens (androstenedione and testosterone) in testicular tissues and in culture medium with or without hCG supplementation. (B) Relative mRNA levels of genes involved in steroidogenesis and androgen/estrogen signaling pathways (normalized to *Gapdh* and *Actb* or to *Hsd3b1*) with or without hCG supplementation. (C) Proportion of seminiferous tubules containing the most advanced type of germ cells after *in vitro* culture with or without hCG. $P < 0.05$: * *vs* 36.5 d*pp* and # *vs* D30 FT. (D) Sertoli cell number in seminiferous tubules after *in vitro* culture with or without hCG.
Data are presented as means ± SEM with n = 4 biological replicates for each group. A value of *$P < 0.05$ was considered statistically significant. FT: Fresh Tissue; CSF: Controlled Slow Freezing.

Fig. 7: Altered steroidogenesis and androgen/estrogen signaling pathways in *in vitro* matured testicular tissues of prepubertal mice A similar density of Leydig cells (LC) is found after 30 days of organotypic culture (D30) and at 36.5 days *postpartum*, the corresponding *in vivo* time point. However, LC are partially mature *in vitro* with a decrease in *Sult1e1* and *Insl3* mRNA levels (adult LC markers). The mRNA levels of *Cyp11a1*, *Cyp17a1* and *Hsd17b3* encoding steroidogenic enzymes and the protein levels of CYP17A1 are decreased *in vitro*. Increased amounts of cholesterol, progesterone and estradiol and decreased androstenedione intratesticular levels are observed at D30. Furthermore, despite testosterone levels similar to *in vivo*, the expression of the androgen receptor (AR) and of the androgen binding protein (*Abp*), androgen signaling is altered at D30, with decreased transcript levels of androgen target genes (*Rhox5*, *Septin12*). Moreover, with severely decreased expression and activity of aromatase and decreased estrogen receptor expression, estrogen signaling is impaired at D30, leading to decreased transcript and protein levels of the estrogen target gene *Faah*.

Supporting information

S1 Fig. Scheme of the study design. At 6.5 d*pp* (D0), the testis contains only spermatogonia and the initiation of meiosis occurs between 7 and 9 d*pp*. At 22.5 d*pp* (D16), meiosis ends and the first round spermatids appear. At 36.5 d*pp* (D30), the first spermatozoa appear and this is the end of the first spermatogenic wave. Arrows represent times at which the medium was collected (D0, D2, D6, D10, D14, D18, D22, D26 and D30).

BM: Basal Medium; CSF: Controlled Slow Freezing; d*pp*: days *postpartum*; hCG: human Chorionic Gonadotropin; KSR: KnockOut Serum replacement; PR-: without phenol red; Rol: retinol

S2 Fig. Impact of controlled slow freezing on Leydig cells in organotypic cultures. (A) Representative images of 3β-HSD expression in Leydig cells (LC) at 6.5 d*pp* and in *in vitro* cultured fresh (FT) or frozen/thawed (CSF) testicular tissues (D16 and D30). Testicular tissue sections were counterstained with Hoechst (blue). Dotted lines delineate seminiferous tubules. Scale: 15 µm. (B) Number of 3β-HSD positive LC per cm² of FT or CSF testicular tissue. (C) Percentage of LC in apoptosis (3β-HSD and cleaved caspase 3 positive) or in proliferation (3β-HSD and Ki67 positive) in *in vivo* and *in vitro* matured FT or CSF tissues. (D) Percentage of 3β-HSD positive LC expressing AR in *in vivo* and *in vitro* matured FT or CSF tissues. (E) Relative mRNA levels of differentiation factors for LC (*Igf1*, *Dhh*), ILC (*Srd5a1*) and of ALC markers (*Sult1e1*, *Insl3*) (normalized to *Gapdh* and *Actb* or to *Hsd3b1*). Data are presented as means ± SEM with n = 4 biological replicates for each group. A value of $*P < 0.05$ was considered statistically significant.

FT: Fresh Tissue, CSF: Controlled Slow Freezing

S3 Fig. **Impact of controlled slow freezing on steroids production by Leydig cells in organotypic cultures.** Concentrations of androgens (androstenedione and testosterone) in the culture medium of fresh (FT) or frozen/thawed (CSF) testicular tissues.

Data are presented as means ± SEM with n = 4 biological replicates for each group. A value of $*P < 0.05$ was considered statistically significant.

S4 Fig. **Impact of different hCG concentrations on testosterone production in organotypic cultures.** (A) Concentrations of testosterone in the culture medium after supplementation with different hCG concentrations (5 pM, 50 pM, 1 nM, 5 nM, 50 nM) from

D16 to D30. (B) Concentrations of testosterone in FT testicular tissues (D30) normalized to *in vivo* control (36.5 d*pp*) and in culture medium at D30 normalized to *in vitro* control without hCG, after supplementation with different hCG concentrations (5 pM, 50 pM, 1 nM, 5 nM, 50 nM).

Data are presented as means ± SEM with n = 4 biological replicates for each group. A value of $*P < 0.05$ was considered statistically significant.

S5 Fig. **Impact of hCG supplementation on mRNA levels of genes involved in steroidogenesis and androgen signaling in organotypic cultures.** Relative mRNA levels of Leydig cell markers, actors of steroidogenesis and androgen signaling (normalized to *Gapdh* and *Actb* or to *Hsd3b1*) after supplementation with 1 nM hCG.

Data are presented as means ± SEM with n = 4 biological replicates for each group. A value of $*P < 0.05$ was considered statistically significant.

S1 Table. Detailed list of antibodies used in this study HRP: horseradish peroxidase; IF: immunofluorescence; IHC: immunohistochemistry; O/N: overnight; RT: room temperature; WB: Western Blot

S2 Table. List of PCR primers used in this study

S3 Table. Compound-specific MRM parameters for LC-MS/MS CE: collision energy; DHEA: Dehydroepiandrosterone; MRM: multiple reaction monitoring

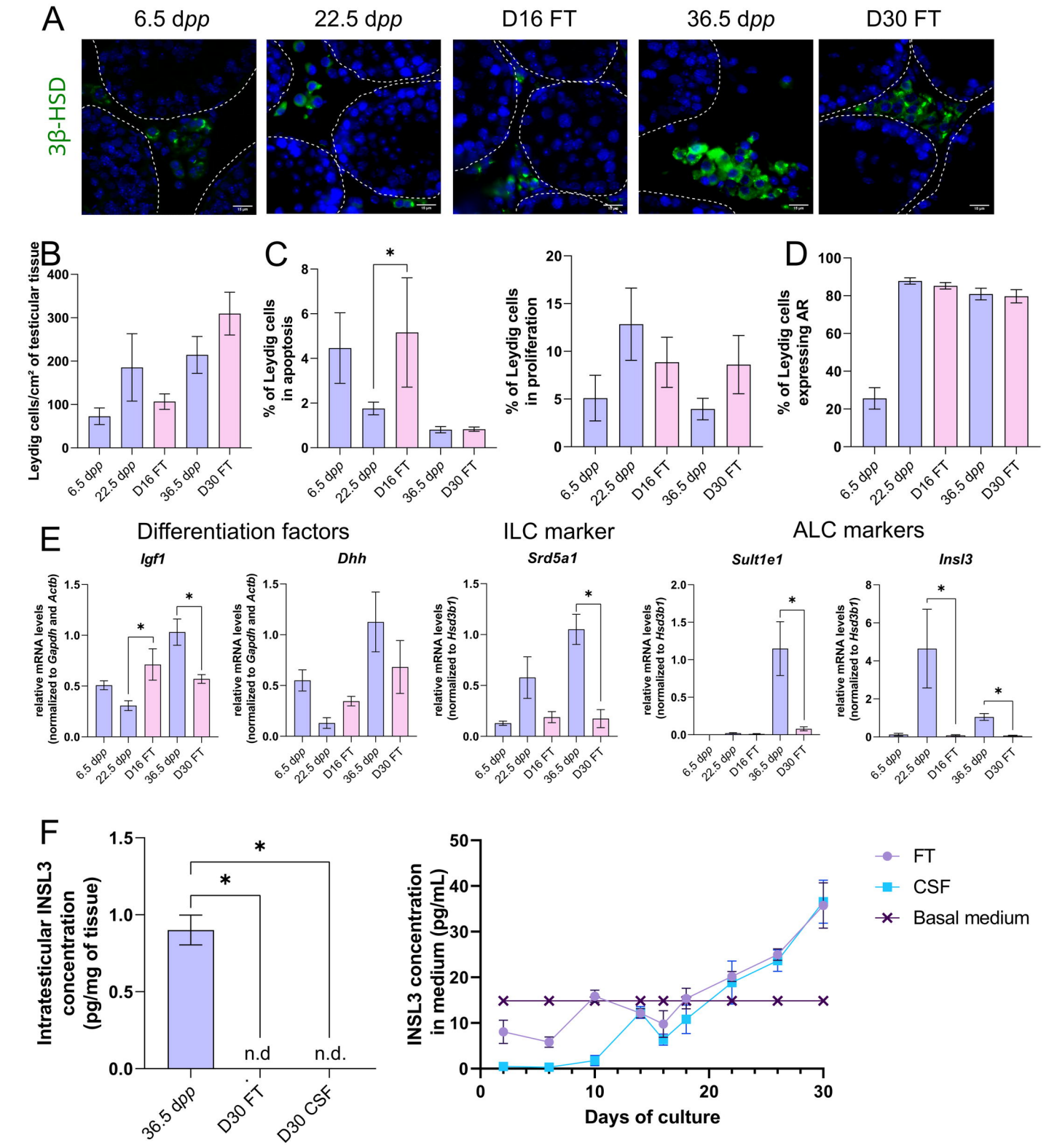
A
6.5 dpp
22.5 dpp
D16 FT
36.5 dpp
D30 FT
3β-HSD
B
Leydig cells/cm² of testicular tissue
C
% of Leydig cells in apoptosis
% of Leydig cells in proliferation
D
% of Leydig cells expressing AR
6.5 dpp
22.5 dpp
D16 FT
36.5 dpp
D30 FT
E
Differentiation factors
ILC marker
ALC markers
Igf1
Dhh
Srd5a1
Sult1e1
Insl3
relative mRNA levels (normalized to Gapdh and Actb)
relative mRNA levels (normalized to Hsd3b1)
F
Intratesticular INSL3 concentration (pg/mg of tissue)
n.d
n.d.
36.5 dpp
D30 FT
D30 CSF
INSL3 concentration in medium (pg/mL)
Days of culture
FT
CSF
Basal medium

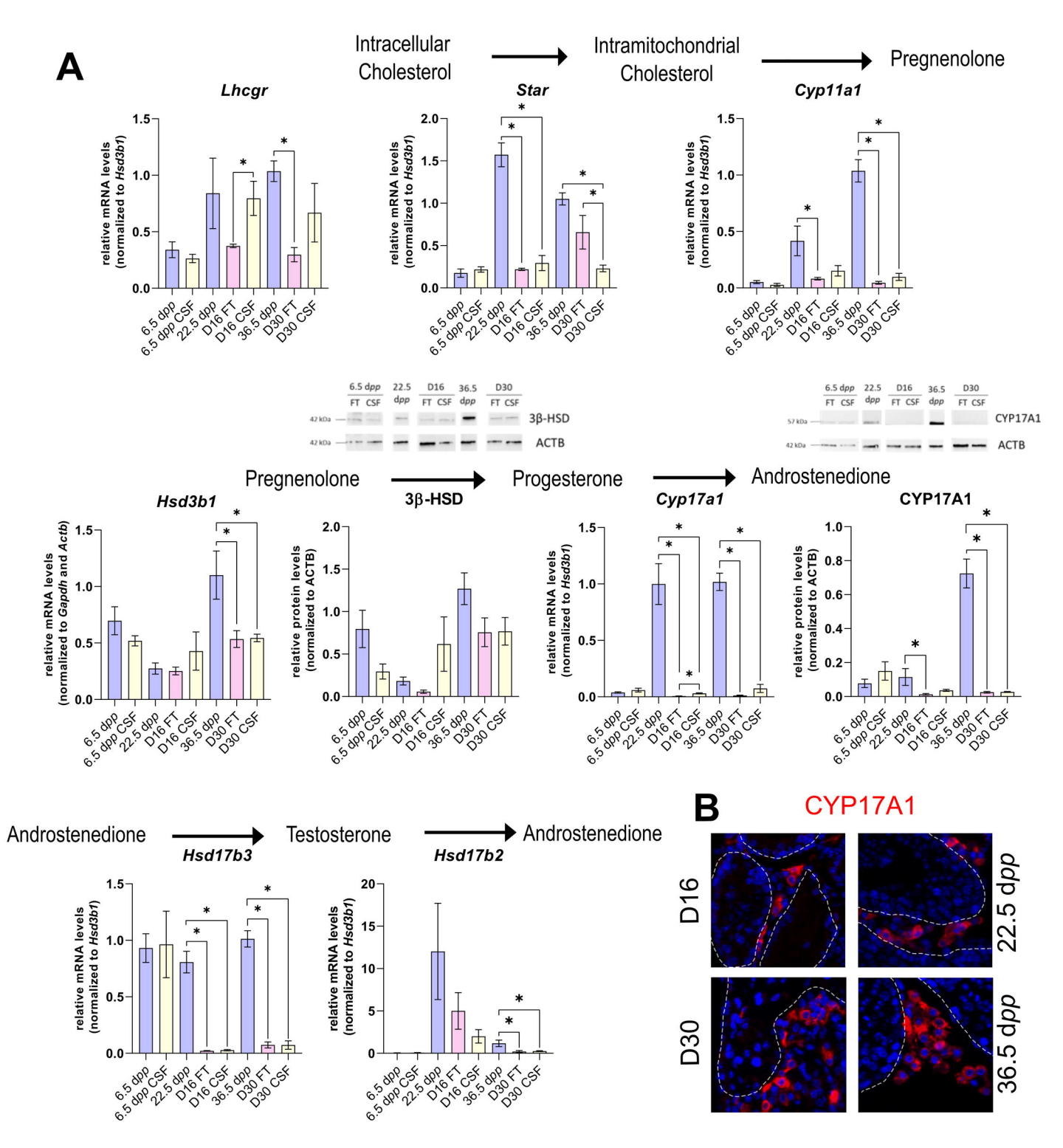
A
Intracellular Cholesterol
Intramitochondrial Cholesterol
Pregnenolone
Lhcgr
Star
Cyp11a1
relative mRNA levels (normalized to Hsd3b1)
6.5 dpp
6.5 dpp CSF
22.5 dpp
D16 FT
D16 CSF
36.5 dpp
D30 FT
D30 CSF
3β-HSD
ACTB
CYP17A1
Pregnenolone
Progesterone
Androstenedione
Hsd3b1
relative mRNA levels (normalized to Gapdh and Actb)
relative protein levels (normalized to ACTB)
Androstenedione
Testosterone
Androstenedione
Hsd17b3
Hsd17b2
B
CYP17A1
D16
D30
22.5 dpp
36.5 dpp

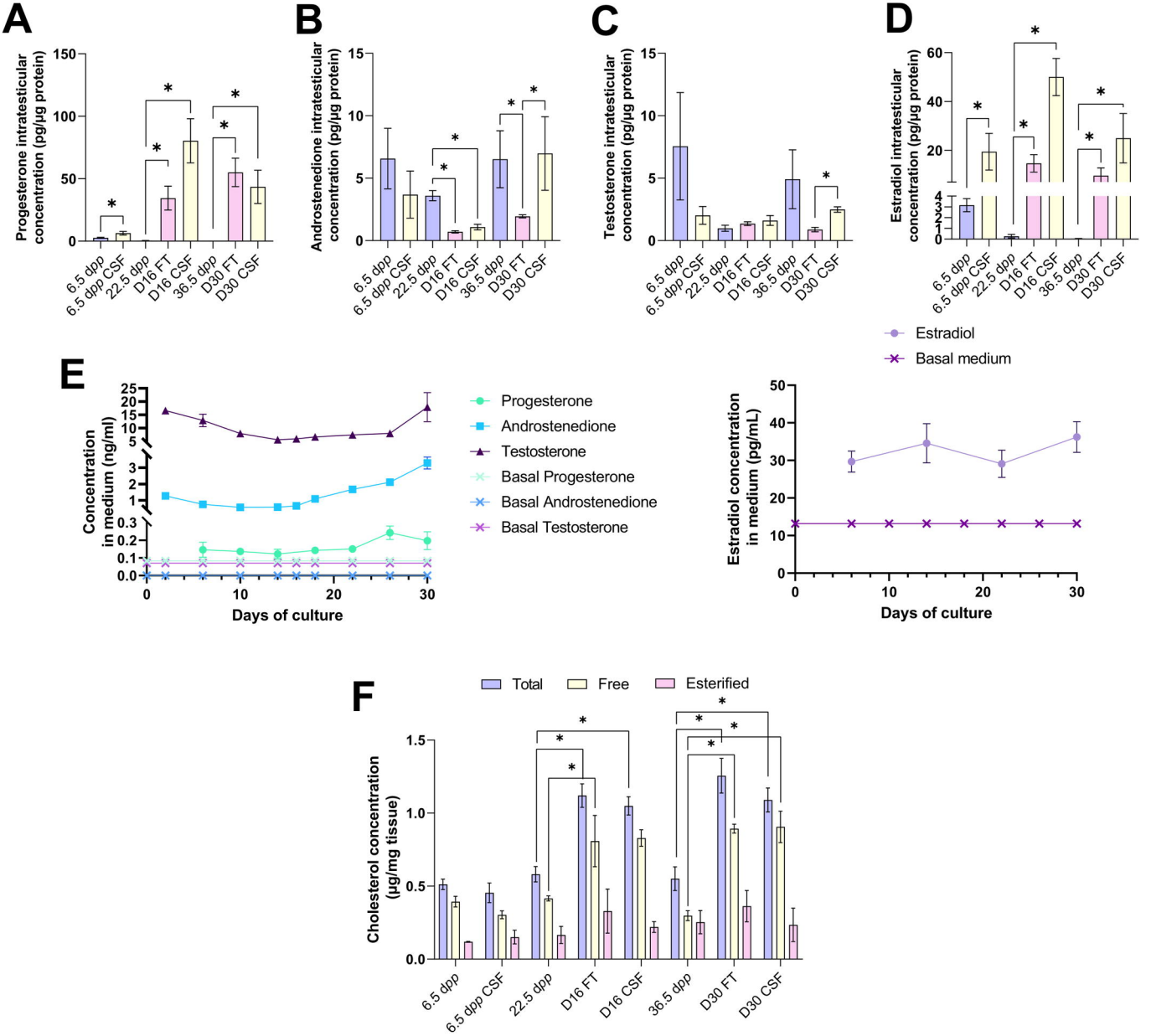
A
Progesterone intratesticular concentration (pg/µg protein)
B
Androstenedione intratesticular concentration (pg/µg protein)
C
Testosterone intratesticular concentration (pg/µg protein)
D
Estradiol intratesticular concentration (pg/µg protein)
6.5 dpp
6.5 dpp CSF
22.5 dpp
D16 FT
D16 CSF
36.5 dpp
D30 FT
D30 CSF
Estradiol
Basal medium
E
Concentration in medium (ng/ml)
Days of culture
Progesterone
Androstenedione
Testosterone
Basal Progesterone
Basal Androstenedione
Basal Testosterone
Estradiol concentration in medium (pg/mL)
Days of culture
F
Total
Free
Esterified
Cholesterol concentration (µg/mg tissue)

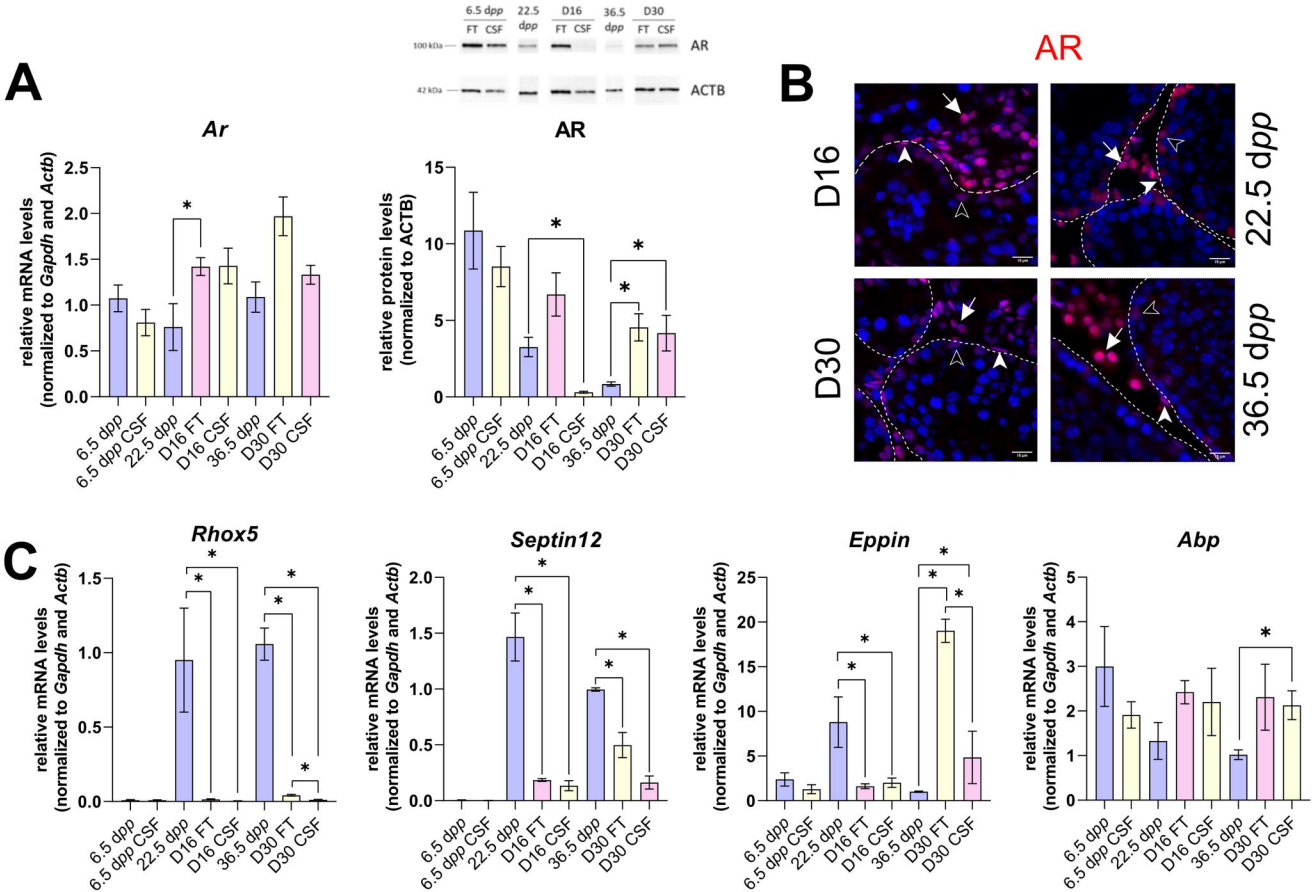
A
6.5 dpp
22.5 dpp
D16
36.5 dpp
D30
FT CSF
100 kDa
42 kDa
AR
ACTB
Ar
relative mRNA levels (normalized to Gapdh and Actb)
AR
relative protein levels (normalized to ACTB)
6.5 dpp
6.5 dpp CSF
22.5 dpp
D16 FT
D16 CSF
36.5 dpp
D30 FT
D30 CSF
B
AR
D16
D30
22.5 dpp
36.5 dpp
C
Rhox5
Septin12
Eppin
Abp

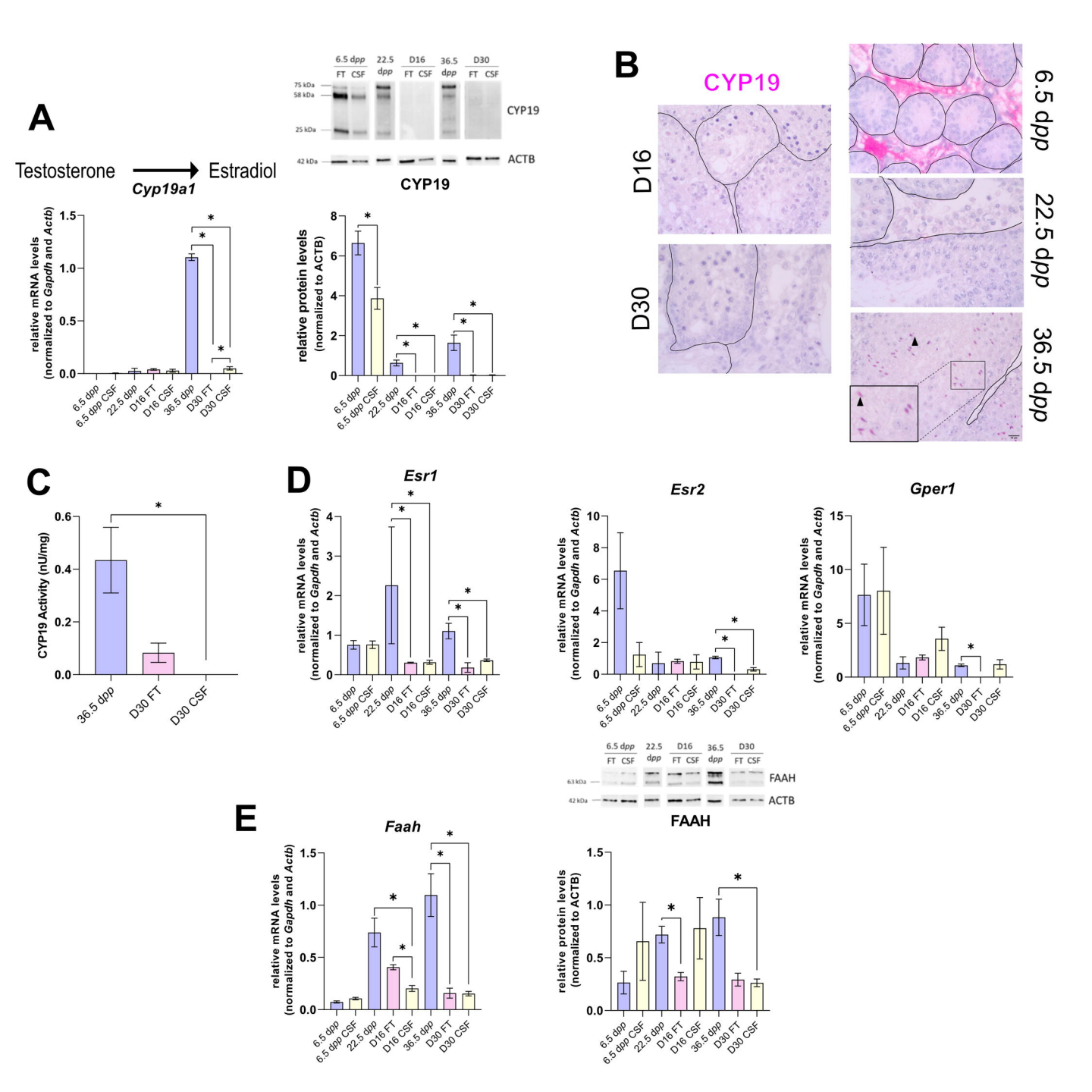
A
Testosterone
Cyp19a1
Estradiol
relative mRNA levels (normalized to Gapdh and Actb)
6.5 dpp
6.5 dpp CSF
22.5 dpp
D16 FT
D16 CSF
36.5 dpp
D30 FT
D30 CSF
6.5 dpp 22.5 dpp D16 36.5 dpp D30
FT CSF FT CSF FT CSF
75 kDa
58 kDa
25 kDa
42 kDa
CYP19
ACTB
CYP19
relative protein levels (normalized to ACTB)
B
CYP19
D16
D30
6.5 dpp
22.5 dpp
36.5 dpp
C
CYP19 Activity (nU/mg)
36.5 dpp
D30 FT
D30 CSF
D
Esr1
Esr2
Gper1
relative mRNA levels (normalized to Gapdh and Actb)
FAAH
ACTB
63 kDa
42 kDa
FAAH
E
Faah
relative mRNA levels (normalized to Gapdh and Actb)
relative protein levels (normalized to ACTB)

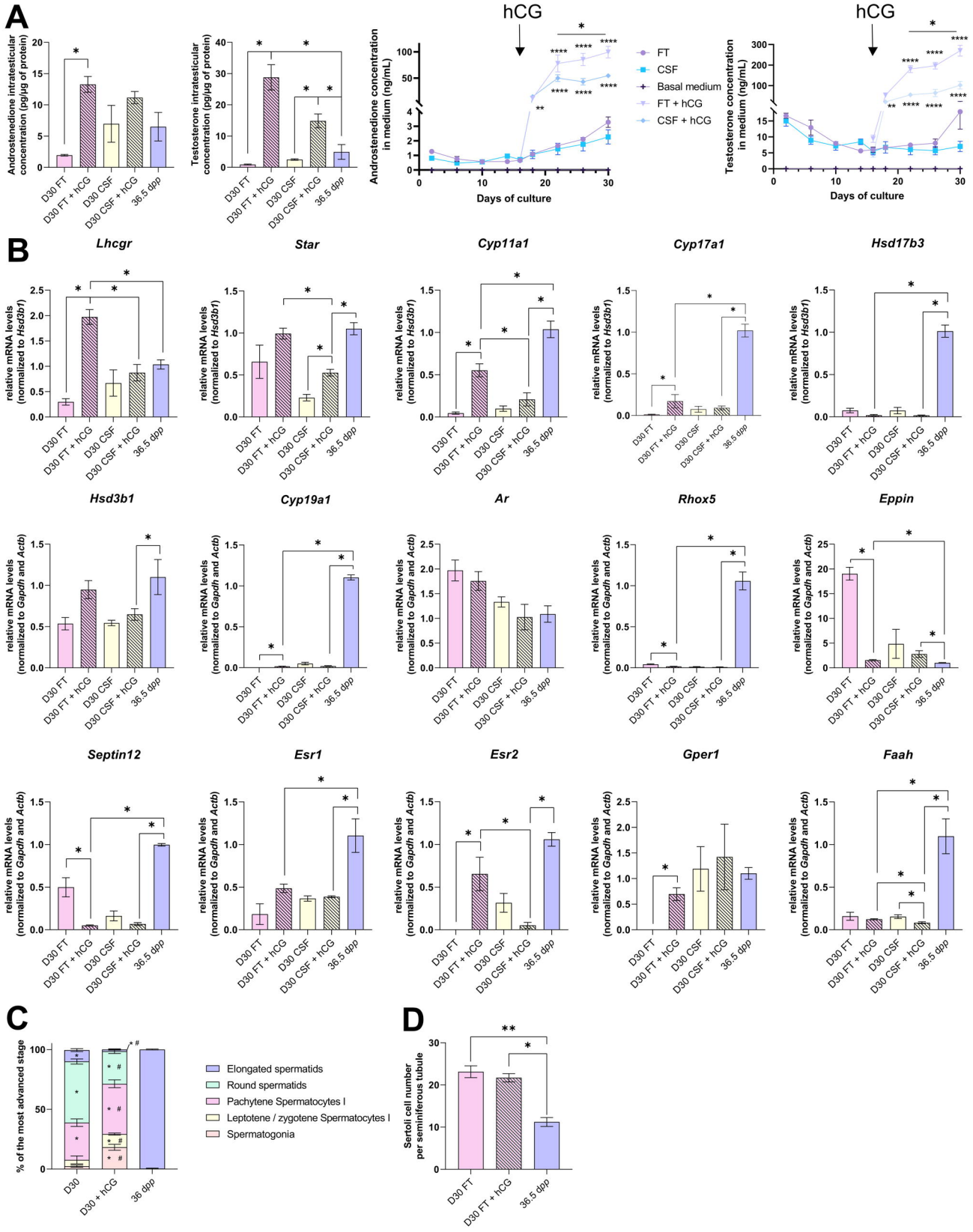
A
Androstenedione intratesticular concentration (pg/µg of protein)
Testosterone intratesticular concentration (pg/µg of protein)
hCG
Androstenedione concentration in medium (ng/mL)
Testosterone concentration in medium (ng/mL)
Days of culture
FT
CSF
Basal medium
FT + hCG
CSF + hCG
D30 FT
D30 FT + hCG
D30 CSF
D30 CSF + hCG
36.5 dpp
B
Lhcgr
Star
Cyp11a1
Cyp17a1
Hsd17b3
Hsd3b1
Cyp19a1
Ar
Rhox5
Eppin
Septin12
Esr1
Esr2
Gper1
Faah
relative mRNA levels (normalized to Hsd3b1)
relative mRNA levels (normalized to Gapdh and Actb)
C
% of the most advanced stage
D30
D30 + hCG
36 dpp
Elongated spermatids
Round spermatids
Pachytene Spermatocytes I
Leptotene / zygotene Spermatocytes I
Spermatogonia
D
Sertoli cell number per seminiferous tubule

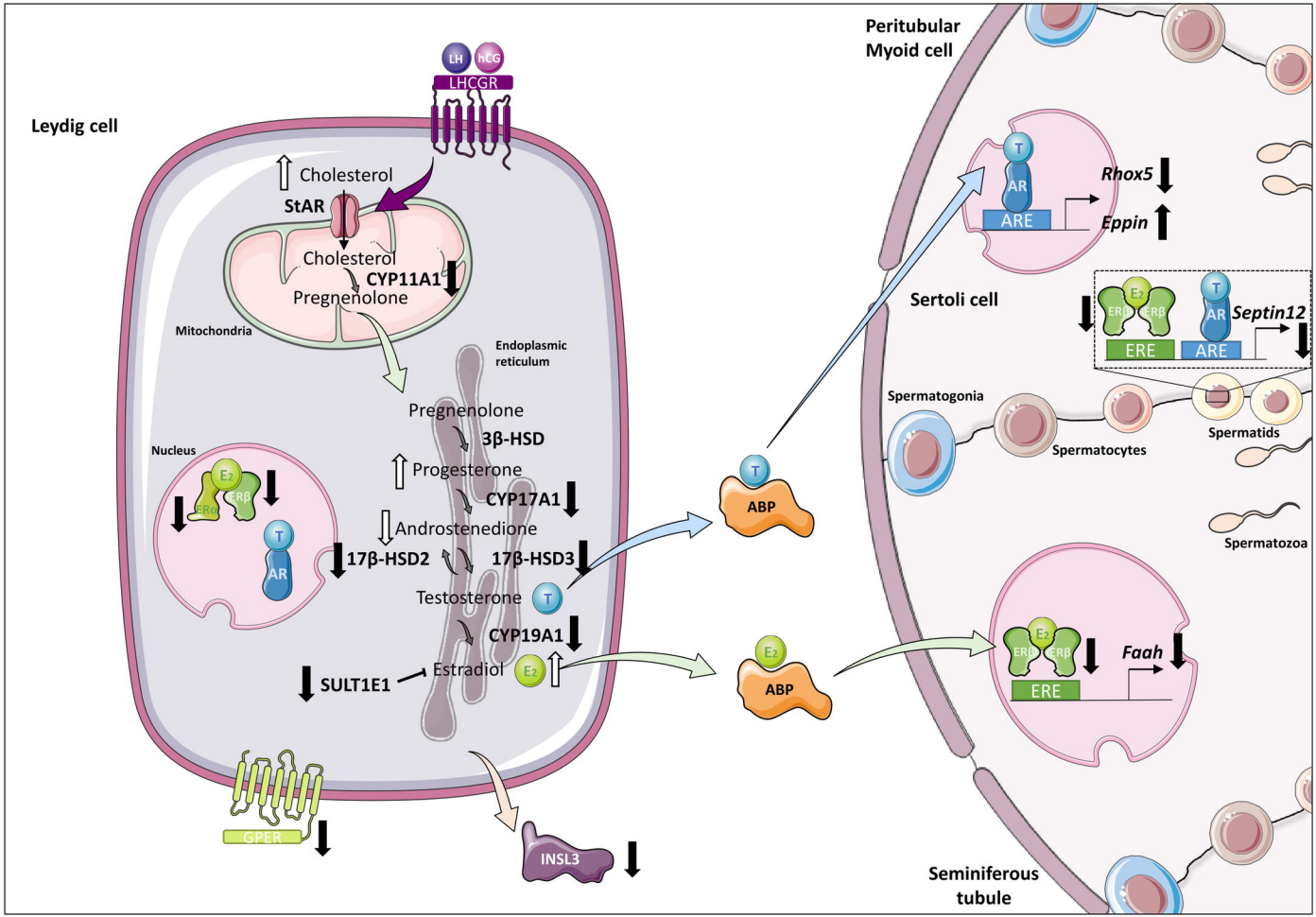
Leydig cell
LH
hCG
LHCGR
Cholesterol
StAR
Cholesterol
CYP11A1
Pregnenolone
Mitochondria
Endoplasmic reticulum
Pregnenolone
3β-HSD
Progesterone
CYP17A1
Androstenedione
17β-HSD2
17β-HSD3
Testosterone
CYP19A1
SULT1E1
Estradiol
Nucleus
E2
ERα
ERβ
T
AR
GPER
INSL3
T
ABP
E2
ABP
Peritubular Myoid cell
T
AR
ARE
Rhox5
Eppin
Sertoli cell
E2
ERα
ERβ
ERE
T
AR
ARE
Septin12
Spermatogonia
Spermatocytes
Spermatids
Spermatozoa
E2
ERα
ERβ
ERE
Faah
Seminiferous tubule